European Journal of Neuroscience, Vol. 12, pp. 2452–2474, 2000

Functional organization of auditory cortex in the Mongolian gerbil (*Meriones unguiculatus*). IV. Connections with anatomically characterized subcortical structures

Eike Budinger, Peter Heil and Henning Scheich
Leibniz Institute for Neurobiology, Brenneckestr. 6, D-39118 Magdeburg, Germany

Keywords: architecture, biocytin, boutons 'en passant', boutons 'terminaux', parvalbumin, rodents

Abstract

The subcortical connections of the four tonotopically organized fields of the auditory cortex of the Mongolian gerbil, namely the primary (AI), the anterior (AAF), the dorsoposterior (DP) and the ventroposterior field (VP), were studied predominantly by anterograde transport of biocytin injected into these fields. In order to allow the localization of connections with respect to subdivisions of subcortical auditory structures, their cyto-, fibre- and chemoarchitecture was characterized using staining methods for cell bodies, myelin and the calcium-binding protein parvalbumin. Each injected auditory cortical field has substantial and reciprocal connections with each of the three subdivision of the medial geniculate body (MGB), namely the ventral (MGv), dorsal (MGd) and medial division (MGm). However, the relative strengths of these connections vary: AI is predominantly connected with MGv, AAF with MGm and MGv, and DP and VP with MGd and MGv. The connections of at least AI and MGv are topographic: injections into caudal low-frequency AI label laterorostral portions of MGv, whereas injections into rostral high-frequency AI label mediocaudal portions of MGv. All investigated auditory fields send axons to the suprageniculate, posterior limitans, laterodorsal and lateral posterior thalamic nuclei, with strongest projections from DP and VP, as well as to the reticular and subgeniculate thalamic nuclei. AI, AAF, DP and VP project to all three subdivisions of the inferior colliculus, namely the dorsal cortex, external cortex and central nucleus ipsilaterally and to the dorsal and external cortex contralaterally. They also project to the deep and intermediate layers of the ipsilateral superior colliculus, with strongest projections from DP and VP to the lateral and basolateral amygdaloid nuclei, the caudate putamen, globus pallidus and the pontine nuclei. In addition, AAF and particularly DP and VP project to paralemniscal regions around the dorsal nucleus of the lateral lemniscus (DNLL), to the DNLL itself and to the rostroventral aspect of the superior olivary complex. Moreover, DP and VP send axons to the dorsal lateral geniculate nucleus. The differences with respect to the existence and/or relative strengths of subcortical connections of the examined auditory cortical fields suggest a somewhat different function of each of these fields in auditory processing.

Introduction

Particularly during the last decade the Mongolian gerbil *(Meriones unguiculatus)* has become a widely used laboratory animal for physiological studies at various levels of the auditory system, including the cochlea (e.g. Echteler *et al*., 1989; Müller, 1996), the cochlear nuclei (e.g. Frisina *et al*., 1990; Feng *et al*., 1994; Ostapoff *et al*., 1994), the superior olivary complex (e.g. Spitzer & Semple, 1995), the inferior colliculus (e.g. Spitzer & Semple, 1991; Brückner & Rübsamen, 1995; Heil *et al*., 1995; Harris *et al*., 1997) and the auditory cortex (e.g. Thomas *et al*., 1993; Scheich *et al*., 1993; Sugimoto *et al*., 1997). The functional organization of the gerbil's auditory cortex is rather complex in that it consists of eight, or possibly more, distinguishable fields, as established by electrophysiological and 2-deoxyglucose metabolic studies (Steffen *et al*., 1988; Caird *et al*., 1991; Scheich *et al*., 1993; Thomas *et al*., 1993; see also Fig. 1). At least four of those fields are tonotopically organized, namely the primary (AI), the anterior (AAF), the dorsoposterior (DP) and the ventroposterior field (VP). In order to get a better understanding of the possible functions of these multiple cortical representations of the receptor surface (cochlea), their afferent and efferent connections need to be studied. In the companion paper (Budinger *et al*., 2000) we have described the architecture of these four tonotopically organized fields of the gerbil's auditory cortex and the cortical connections. Here we examine their subcortical connections by means of the predominantly anterograde but also retrograde transport of the sensitive tracer biocytin. Corticofugal projections can modulate the response characteristics of neurons in the target areas (e.g. Ryugo & Weinberger, 1976; Villa *et al*., 1991; Yan & Suga, 1998). Hence, the present and further studies may help to advance our knowledge of the anatomical basis of these descending influences. We also provide a relatively coarse description of the cyto-, myelo- and chemoarchitecture of the ascending auditory pathway. This survey only serves to allow the localization of projections from the auditory cortex with respect to major subdivisions of the auditory nuclei and to provide a basis for future, more detailed, studies of these projections and their target areas.

Some of the present data have been published in abstract form (Budinger & Scheich, 1997).

Correspondence: Dr Eike Budinger, Leibniz Institute for Neurobiology, PO Box 1860, D-39008 Magdeburg, Germany.
E-mail: budinger@ifn-magdeburg.de

Received 25 November 1999, revised 6 April 2000, accepted 10 April 2000

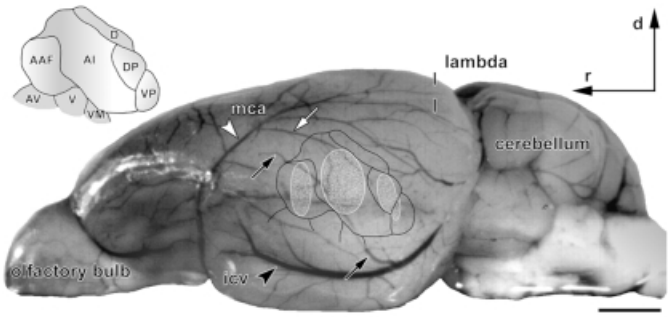

FIG. 1. Placements of injections into primary auditory field (AI), anterior auditory field (AAF), dorsoposterior auditory field (DP) and ventroposterior auditory field (VP) (white shaded areas) were made according to stereotaxic coordinates relative to lambda and to conspicuous features of the cortical vasculature. For example, the boundary between AI and AAF is located close to a distinctive ascending branch (black arrows) of the inferior cerebral vein (icv) and the dorsal border of AI is located near a distinctive descending branch (white arrow) of the middle cerebral artery (mca; Hess & Scheich, 1996; Sugimoto *et al*., 1997). Upper right inset shows a functional map of the gerbil's auditory cortex which is superimposed onto the cortical surface. Scale bar, 2.0 mm.

Materials and methods

Animals

Forty-seven young adult male Mongolian gerbils (*Meriones unguiculatus*), which were at least four months old and weighed 80–100 g, were used for the present study. The methods are largely identical to those in the companion paper (Budinger *et al*., 2000) and are therefore described here only briefly.

Histology

In order to unequivocally assign the biocytin label to subcortical structures, their cyto-, myelo- and chemoarchitecture was studied. For this purpose, 12 gerbils were deeply anaesthetized (0.5 mg ketamine/100 g body weight and 0.3 mg xylazine/100 g body weight, i.p.) and perfused transcardially with 200 mL Ringer solution (pH 7.4), containing 0.5% heparin, followed by 200 mL of 4% paraformaldehyde and 0.1% glutaraldehyde in 0.05 M phosphate buffer (pH 7.4). The brains were removed and stored overnight at 4 °C and then cut on a vibratome into series of frontal or horizontal sections of 60-μm thickness. The sections of four brains each, three cut in the frontal and one in the horizontal plane, were stained for cell bodies (Nissl substance), myelinated fibres and the calcium-binding protein parvalbumin (PV). Cell bodies were stained with cresyl violet and myelinated fibres according to the silver staining method of Gallyas (1979). To visualize PV, sections were first incubated in a solution containing the PV antibody (Sigma Chemicals, Germany, dilution of 1 : 4000, 48 h) and 0.1% Triton. Thereafter, the PV antibody was recognized by a secondary antibody (biotinylated anti-mouse, Sigma Chemicals, dilution of 1 : 200, 2 h) and visualized using the avidin-biotin-peroxidase method (ABC-kit, Vector Laboratories, CA, USA) with diaminobenzidine or α-chloronaphtol as chromogen.

Tracing experiments

To study the subcortical connections by means of biocytin (Sigma Chemicals), 35 gerbils were anaesthetized (0.4 mg ketamine/100 g body weight and 0.3 mg xylazine/100 g body weight, i.p.). The skin over the left temporal cortex was incised and a small hole drilled into the skull. In each animal, 0.1 μL of biocytin (5% in 0.05 M TRIS buffer, pH 7.6) was injected by pressure over a period of two minutes using fine glass micropipettes mounted on a nanoinjector. Each injection was performed into selected parts of the left auditory cortex using stereotaxic coordinates and conspicuous landmarks of the surface vasculature, as described in great detail in the companion paper (Budinger *et al*., 2000). Figure 1 illustrates the areas where the injections were positioned with respect to the typical surface vasculature of the gerbil's brain. The upper right inset (modified from Thomas *et al*., 1993) demonstrates the relative location of auditory cortical fields to each other. The outlines are also superimposed onto the cortical surface. Fifteen injections were made into AI, ten into AAF, eight into DP and two into VP. Injections into AI were deliberately placed at different rostrocaudal positions. Positions of the injections were verified and further specified after histological processing of the brains using reliable internal anatomical landmarks such as the rostral pole of the hippocampus and the dorsal roof of the caudate putamen (see Budinger *et al*., 2000; Fig. 5D–F). After closing the surgical opening the animals survived for 24 h and were then reanaesthetized (0.5 mg ketamine/100 g body weight and 0.3 mg xylazine/100 g body weight, i.p.) and perfused transcardially with 200 mL Ringer solution (pH 7.4), containing 0.5% heparin, followed by 200 mL of 4% paraformaldehyde and 0.1% glutaraldehyde in phosphate buffer (pH 7.4). The brains were stored overnight at 4 °C and then cut on a vibratome into frontal (six AI-injected brains, four AAF, three DP, one VP) or horizontal sections (nine AI, six AAF, five DP, one VP) of 60-μm thickness. In order to visualize the anterograde and retrograde transport of biocytin the sections were processed according to the methods of King *et al*. (1989) and Izzo (1991) using the ABC-peroxidase reaction (Vector Laboratories) with diaminobenzidine (mostly nickel-intensified) as chromogen. The sections were mounted, counterstained (methylgreen), dehydrated and coverslipped. In addition, selected sections were counterstained for cell bodies or PV, as described above, to correlate the tracing and the anatomical data.

All sections were microscopically analysed (Leica/Leitz DMR-system, Germany) and regions of interest were photographed. Computer-scanned (Agfa Arcus II, Germany) photographs were arranged for illustrations using the Adobe Photoshop software for Macintosh.

The general nomenclature used in this study largely corresponds to the rat stereotaxic atlas (Paxinos & Watson, 1986) and description (Paxinos, 1995) and to the gerbil stereotaxic atlas (Loskota *et al*., 1974).

The experiments were approved by the animal ethics committee of Sachsen-Anhalt (No. 53a-42502/2–161 IFN MD) in accordance to the NIH Guide for the Care & Use of Laboratory Animals (1996).

Results

Cyto-, myelo- and chemoarchitecture of auditory subcortical structures

The auditory thalamus

Figure 2A–C shows three frontal sections through the thalamus at about the same rostrocaudal level illustrating the staining patterns of the medial geniculate body (MGB) and surrounding structures for cell bodies (Nissl stain, Fig. 2A), myelinated fibres (Gallyas stain, Fig. 2B) and PV (Fig. 2C). The schematic drawing in Fig. 2D illustrates the outlines of the three major subdivisions of the MGB, namely the ventral (MGv), medial (MGm) and dorsal (MGd) division, as they were derived from these stains.

The Nissl stain (Fig. 2A) reveals that the MGv, which constitutes the largest subdivision, is tightly packed with small- and medium-

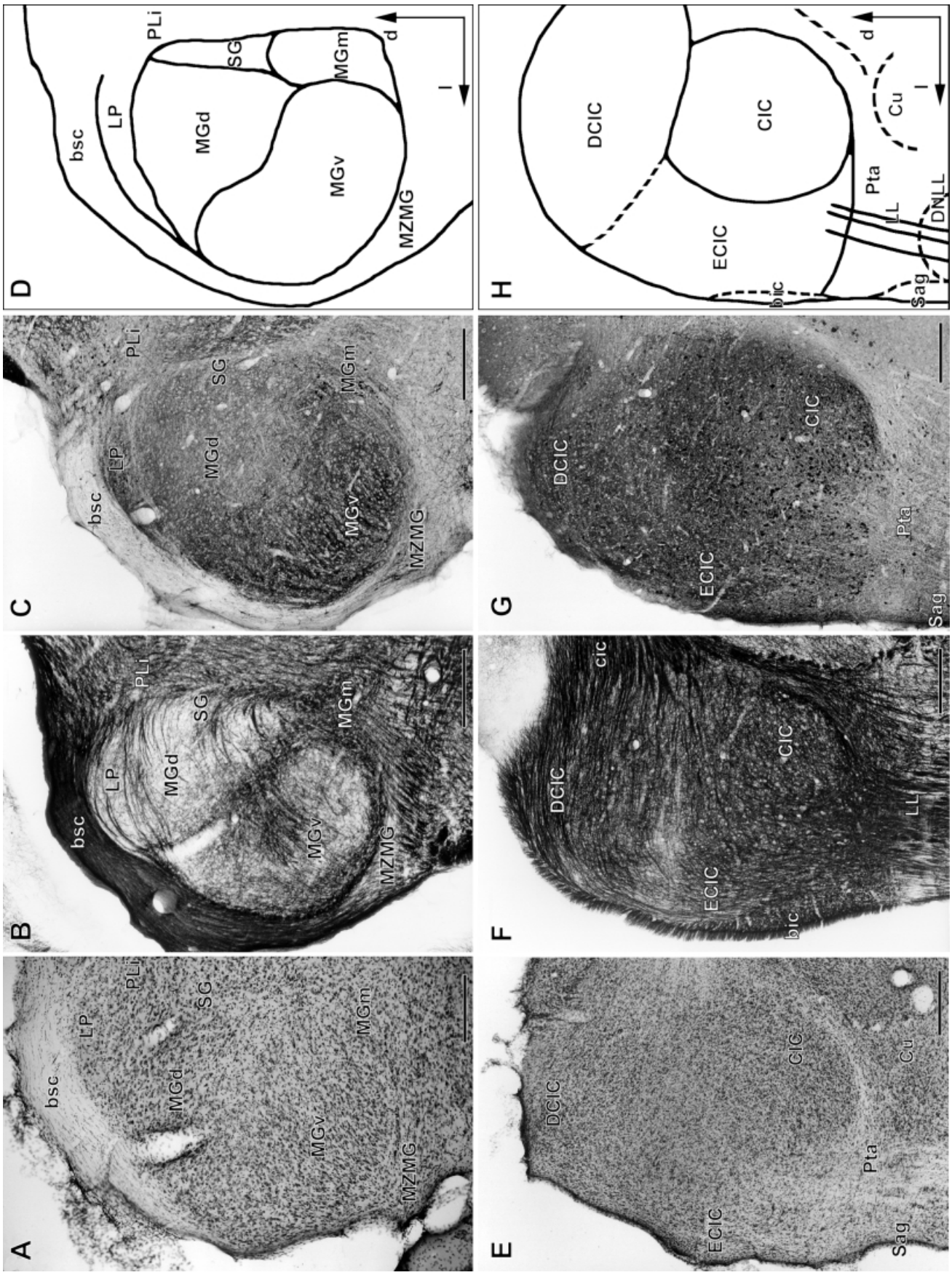
A
B
C
D
E
F
G
H
bsc
LP
PLi
SG
MGd
MGv
MGm
MZMG
d
l
DCIC
ECIC
CIC
Pta
Cu
Sag
cic
bic
LL
DNLL

sized neurons. The neurons in the MGd have a similar size, but are more loosely packed. The largest neurons (so-called 'magnocellular' neurons) are found in the MGm where they are most numerous in the caudal part. The suprageniculate nucleus (SG) can be identified dorsal to the MGm and medial to the MGd. The SG is distinguished from the MGd by the slightly larger size of its neurons and their lower packing density. Medial to the SG, the posterior limitans thalamic nucleus (PLi) forms a vertical column and extends dorsally to the anteroventral border of the superior colliculus (SC). The orientation of myelinated fibres divides the MGB predominantly into its ventral and dorsal division (Fig. 2B). Both subdivisions are less intensely stained for myelin than is the MGm, which is characterized by a dense plexus of stained fibres. Within the SG, fibre bundles are largely orientated horizontally. Their intersections with vertically orientated fibres approximately mark the border between the SG and the PLi. The immunoreactivity against PV predominates in the MGv and MGm (Fig. 2C). In the MGv, the antibody recognizes predominantly terminal-like structures (boutons and fibres) causing the densely stained neuropil of this nucleus. Immunopositive somata are rare and loosely distributed. In the MGm, the somata, dendrites and axonal elements of large- and medium-sized cells of various shapes are labelled. The MGd and SG exhibit similar staining patterns and thus are not clearly distinguishable from each other but the PV immunoreactivity is less than in the MGv and MGm.

The inferior colliculus (IC)

The cyto-, myelo- and chemoarchitectural staining patterns reveal a parcellation of the inferior colliculi into three subdivisions (Fig. 2E–H), namely a large central nucleus (CIC), located at the medioventral aspect of the IC, a dorsal cortex (DCIC), extending dorsally close to the SC, and an external cortex (ECIC), occupying the lateral aspect of the IC.

The orientation and distribution of Nissl-stained cell bodies (Fig. 2E) allow the distinction of an oval area of densely packed large, medium-sized and small neurons, the CIC, a dorsal area of more loosely packed neurons of various size, the DCIC, and a lateral area of loosely packed neurons, the ECIC. The DCIC and ECIC have a laminated appearance with cell size increasing towards deeper layers. The tectal structures of the IC are largely surrounded by tegmental nuclei (see Morest & Oliver, 1984). Using the Nissl stain we could distinguish particularly the cuneiform nucleus (Cu), which is located within the medioventral pericollicular tegmental area, and the lateroventrally located nucleus sagulum (Sag). In the myelin stain (Fig. 2F) the CIC is characterized by a dense plexus of fibres orientated in a dorsomedial to ventrolateral direction. Within the DCIC, myelinated fibres course predominantly horizontally, and within the ECIC, vertically. The outer layers of both subdivisions merge into one another and form a capsule wrapping the CIC and continuing into the commissure of the IC mediodorsally and into the brachium of the IC laterally. The fibres of the lateral lemniscus (LL) enter the IC ventrally. PV immunoreactivity of the neuropil (Fig. 2G) is intense throughout the entire IC and just slightly paler in the outer layers of the ECIC and DCIC. A large number of PV-positive terminal-like puncta can be observed in all subdivisions of the IC. The PV antibody labels somata of neurons, but rarely their dendrites, in all subdivisions of the IC but primarily in the CIC. Here, labelled neurons have various sizes and shapes, and probably include both disc-shaped and stellate cells (Rockel & Jones, 1973a; Oliver & Morest, 1984; Faye-Lund & Osen, 1985). Within the ECIC and DCIC, labelled neurons have somata of multipolar shape and primarily large to medium size.

The nuclei of the lateral lemniscus (NLL)

The NLL form an elongated structure on the lateral brainstem extending from the superior olivary complex to the IC. Three subdivisions of the NLL can be identified, namely a dorsal (DNLL), an intermediate (INLL) and a ventral (VNLL) nucleus of the lateral lemniscus (Fig. 3A–D). The latter consists of a compact ventral (vVNLL) and an elongated dorsal part (dVNLL). The nuclei are interspersed with the thick fibre bundles of the LL.

In the Nissl stain (Fig. 3A), the DNLL, INLL and vVNLL can be recognized as groups of cells of various size, each group forming an oval nucleus. The dVNLL, located between the INLL and vVNLL, is characterized by its column-like arrangement of neurons in the frontal plane. In frontal sections (Fig. 3B) myelin-stained fibres are primarily orientated in a dorsoventral direction within the NLL, forming a more complex pattern in the vVNLL and DNLL than in the INLL or dVNLL. Dorsally, the fibres of the LL enter the IC. The PV immunoreactivity is strong within the entire NLL (Fig. 3C). Thick axons, terminal-like puncta, somata and proximal dendritic aspects of neurons of various sizes were PV-positive. In the DNLL we found cells of large, medium and small size and of round, ovoid and elongated shape, similar to those described in cat and rat (Kane & Barone, 1980; Bajo *et al*., 1993). Within the INLL a few PV-positive neurons of multipolar and horizontally elongated shape (Glendenning *et al*., 1981) were found. In the VNLL, immunoreactive cells have various shapes (globular, multipolar, vertically elongated) and sizes (Schofield & Cant, 1997).

The superior olivary complex (SOC)

Four subdivisions of the SOC can be easily distinguished (Fig. 3E–H), namely the lateral (LSO) and medial (MSO) superior olive, the medial nucleus of the trapezoid body (MNTB) and the superior periolivary nucleus (SPN). They are surrounded by various more inconspicuous, loosely organized periolivary cell groups including (according to Schwartz, 1992; see Fig. 3H) a ventral nucleus of the trapezoid body (VNTB) ventral and medial to the MSO, a lateral nucleus of the trapezoid body (LNTB) ventral to the LSO, a lateroventral periolivary nucleus (LVPO) between the LSO and MSO, a medioventral periolivary nucleus (MVPO) between the MSO and MNTB, a dorsal periolivary nucleus (DPO) between the LSO and SPN, a dorsolateral periolivary nucleus (DLPO) dorsal to the LSO, a rostral periolivary nucleus (RPO, see Fig. 3C) at the rostral aspect of the SOC and a caudal periolivary nucleus (CPO) at its caudal pole.

In frontal Nissl-stained sections (Fig. 3E) the LSO appears kidney-shaped and contains large to small, relatively densely packed

FIG. 2. Frontal sections showing the cyto-, myelo- and chemoarchitecture of the medial geniculate body (MGB) and inferior colliculus (IC). Orientation is given in D and H. (A–C) Nissl stain (A), myelin stain (B) and immunoreactivity against parvalbumin (C) delineate the three major subdivisions of the MGB, namely the ventral (MGv), dorsal (MGd) and medial part (MGm), as well as the suprageniculate nucleus (SG). (D) Schematic drawing illustrating major outlines of the MGB and surrounding structures. (E–G) Nissl stain (E), myelin stain (F) and immunoreactivity against PV parvalbumin (G) of the IC at a rather rostral level. The three major subdivisions of the IC are indicated: a central nucleus (CIC), an external cortex (ECIC) and a dorsal cortex (DCIC). (H) Schematic drawing illustrating major outlines of the IC. The absolute and relative size of the CIC is larger at more caudal levels. Scale bars, 300 µm.

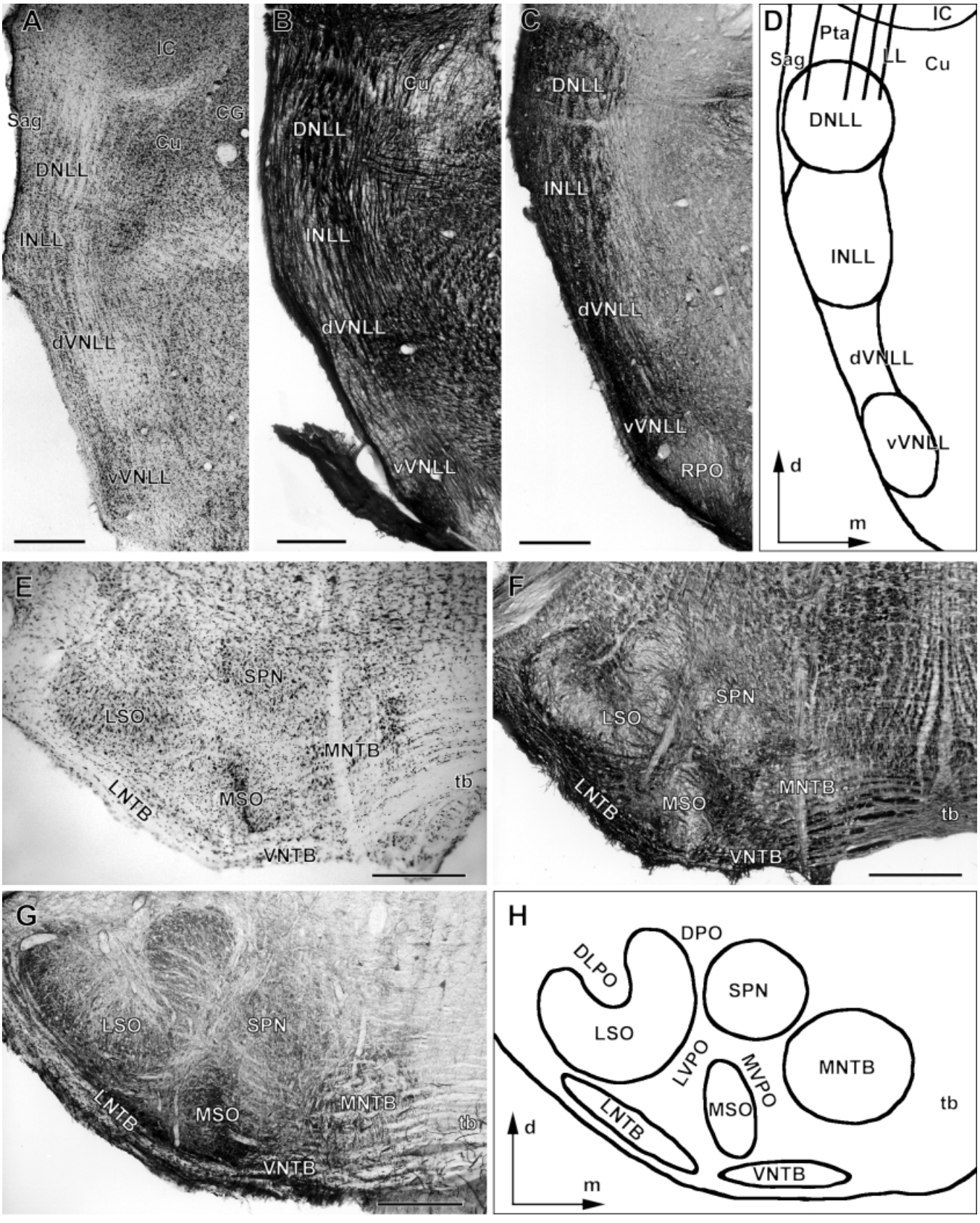
A
IC
Sag
CG
Cu
DNLL
INLL
dVNLL
vVNLL
B
Cu
DNLL
INLL
dVNLL
vVNLL
C
DNLL
INLL
dVNLL
vVNLL
RPO
D
IC
Pta
Sag
LL
Cu
DNLL
INLL
dVNLL
vVNLL
d
m
E
SPN
LSO
MNTB
LNTB
MSO
tb
VNTB
F
SPN
LSO
LNTB
MSO
MNTB
tb
VNTB
G
LSO
SPN
LNTB
MSO
MNTB
tb
VNTB
H
DPO
DLPO
SPN
LSO
LVPO
MVPO
MNTB
MSO
LNTB
tb
d
m
VNTB

neurons. The MSO appears as a vertical column of tightly packed neurons, whereas the MNTB and SPN form large oval aggregates of moderately densely packed neurons. Within the other periolivary nuclei, neurons are more loosely packed. The shapes and sizes of cells vary over wide ranges, but the highest numbers of large cells are found in the MSO, SPN, MNTB and LSO. Myelinated fibres wrap the LSO, MSO, SPN and MNTB (Fig. 3F). The orientation of fibres emphasizes the shapes of these nuclei. The other nuclei of the SOC are difficult to distinguish from each other in myelin-stained sections due to their dense and diffuse network of fibres. All nuclei of the SOC contain heavily stained PV-positive neuronal elements, making the SOC easily distinguishable from the adjacent brainstem structures (Fig. 3G). The highest densities of immunoreactive somata can be found in the MSO, LNTB, MNTB and LSO. PV-positive neurons in these subdivisions have various shapes and sizes. In the LSO, small to large cells have either a round, an elongated or a multipolar appearance (Helfert & Schwartz, 1986, 1987). In the MSO large multipolar and bipolar as well as elongated cells of various sizes (Schwartz, 1977, 1992) contain PV. In the MNTB round cells of various sizes and large multipolar neurons (Morest, 1968; Schwartz, 1992) are found. Within the LNTB strongly PV-labelled neurons are medium-sized to large. Many, but paler stained, PV-positive somata are also found in the SPN, where they have a large multipolar appearance. PV-positive fibres are scattered throughout the entire SOC and display a similar pattern to the myelin stain. Most heavily labelled PV-positive fibres are found within the VNTB and the MNTB.

The cochlear nuclei (CN)

Three major divisions of the CN complex are conspicuous: an anteroventral (AVCN), a posteroventral (PVCN) and a dorsal (DCN) cochlear nucleus (Fig. 4).

The AVCN is characterized by its predominantly large neurons (Fig. 4A). In the rostrodorsal AVCN (spherical cell area) neurons are somewhat smaller and more densely packed than in the caudoventral AVCN (globular cell area). The PVCN (Fig. 4E), separated from the AVCN by the auditory nerve root, comprises a rostroventral region (globular cell area) of higher and a caudodorsal region (octopus cell area) of lower cell packing density, respectively. Cell size within the PVCN varies from very large to small. The DCN (Fig. 4E) appears as a layered structure separated from the ventral complex by the acoustic stria. Four layers are conspicuous. The outermost layer 1 contains small, loosely packed neurons, and is well separable from layer 2, which is most densely packed with predominantly medium-sized to large cells. Laterally, layer 2 is continuous with a band of small cells which form the superficial granule cell layer. This layer covers the dorsal and lateral surface of the ventral cochlear complex. The deeper layers 3 and 4 of the DCN contain very large to small cells slightly less densely packed in layer 4 than layer 3. In the myelin stain (Fig. 4B and F), the fibres of the auditory nerve, the trapezoid body and acoustic stria are the most obvious fibre tracts of the CN complex. The auditory nerve enters the AVCN from a rostroventral direction, bifurcates, and the ascending branch innervates the anterior nucleus. The PVCN is characterized by dense myelin staining caused by the fibres of the descending nerve branch. In the DCN, the four layers are clearly distinguishable in myelin-stained frontal sections. The density of myelinated fibres increases from the outermost layer 1 to the innermost layer 4. The PV antibody heavily stains the neuropil in the CN (Fig. 4C and G) delineating the borders between the major subdivisions. Fibres of the auditory nerve, acoustic stria and trapezoid body are moderately stained, with strongest labelling of thick axons. The PV-positive somata and in some cases also proximal dendritic aspects probably correspond to a variety of cell types (Hackney *et al.*, 1990; Cant, 1992). Within the AVCN large and small ovoid and multipolar cells of various sizes are labelled. Within the PVCN small to very large multipolar cells in the octopus cell area and large ovoid and small to very large multipolar cells in the globular cell area are labelled. Just a few PV-positive, small- to medium-sized, round to elongated cells are found in layers 1 and 2 of the DCN. Layers 3 and 4 of the DCN contain mainly small- to medium-sized multipolar and elongated PV-positive neurons.

Subcortical connections of auditory cortex

General observations

We found a variety of projections terminating in the pros-, mes- and metencephalon following injections of biocytin into each of the four tonotopically organized fields of the gerbil auditory cortex, namely AI, AAF, DP and VP. The anterograde transport of biocytin allowed us to trace the complete direct pathways from the injection site in the auditory cortex via fibre tracts and outbranchings of axons and collaterals to the projection areas. There, we observed two kinds of synaptic contacts, i.e. boutons 'en passant' and boutons 'terminaux'. Generally, labelled axons left the injection site perpendicular to the cortical layers and entered the external capsule as a thick fibre bundle (see Fig. 5A). Here, interhemispheric axons turned dorsally and ventrally, towards the corpus callosum and the anterior commissure, respectively. A third arm left the external capsule ventrally towards the amygdaloid complex but the main bundle turned medially to split into a corticostriatal and a corticothalamic/corticopeduncular branch. The former terminated within the caudate putamen (CPu) and globus pallidus (GP), the latter entered the internal capsule. The corticothalamic branch left the internal capsule medially towards the thalamus. Here, some axons terminated within the reticular (Rt) and subgeniculate (SubG) thalamic nuclei while others reached, via the superior thalamic radiation, the MGB complex and other thalamic nuclei. Although difficult to distinguish at the light microscopic level, at least some of the axons terminating in the CPu/GP, Rt and SubG appeared to be collaterals of parental corticothalamic fibres. Within the internal capsule, the corticopeduncular axons traveled ventrocaudally via the cerebral peduncle and longitudinal fasciculus pons towards the pontine nuclei and the SOC, whereas other axons formed the corticocollicular and corticolemniscal pathways. Axons terminating in the SC and IC passed via the brachii of the SC and of the IC,

FIG. 3. Frontal sections showing the cyto-, myelo- and chemoarchitecture of the nuclei of the lateral lemniscus (NLL) and superior olivary complex (SOC). Orientation in D and H. (A–C) Nissl stain (A), myelin stain (B) and immunoreactivity against parvalbumin (C) of the NLL allow the distinction of a dorsal (DNLL), an intermediate (INLL) and a ventral nucleus (VNLL). The latter can be divided into a dorsal (dVNLL) and a ventral part (vVNLL). (D) Schematic drawing illustrating major outlines of subdivisions of the NLL. (E–G) Nissl stain (E), myelin stain (F) and immunoreactivity against parvalbumin (G) allow the distinction of several subdivisions of the SOC: the lateral (LSO) and medial superior olive (MSO), the medial (MNTB), ventral (VNTB) and lateral nucleus of the trapezoid body (LNTB) and the superior (SPN), dorsal (DPO), dorsolateral (DLPO), lateroventral (LVPO) and medioventral periolivary nucleus (MVPO). (H) Outline diagram illustrating major subdivisions of the SOC. Scale bars, 300 μm.

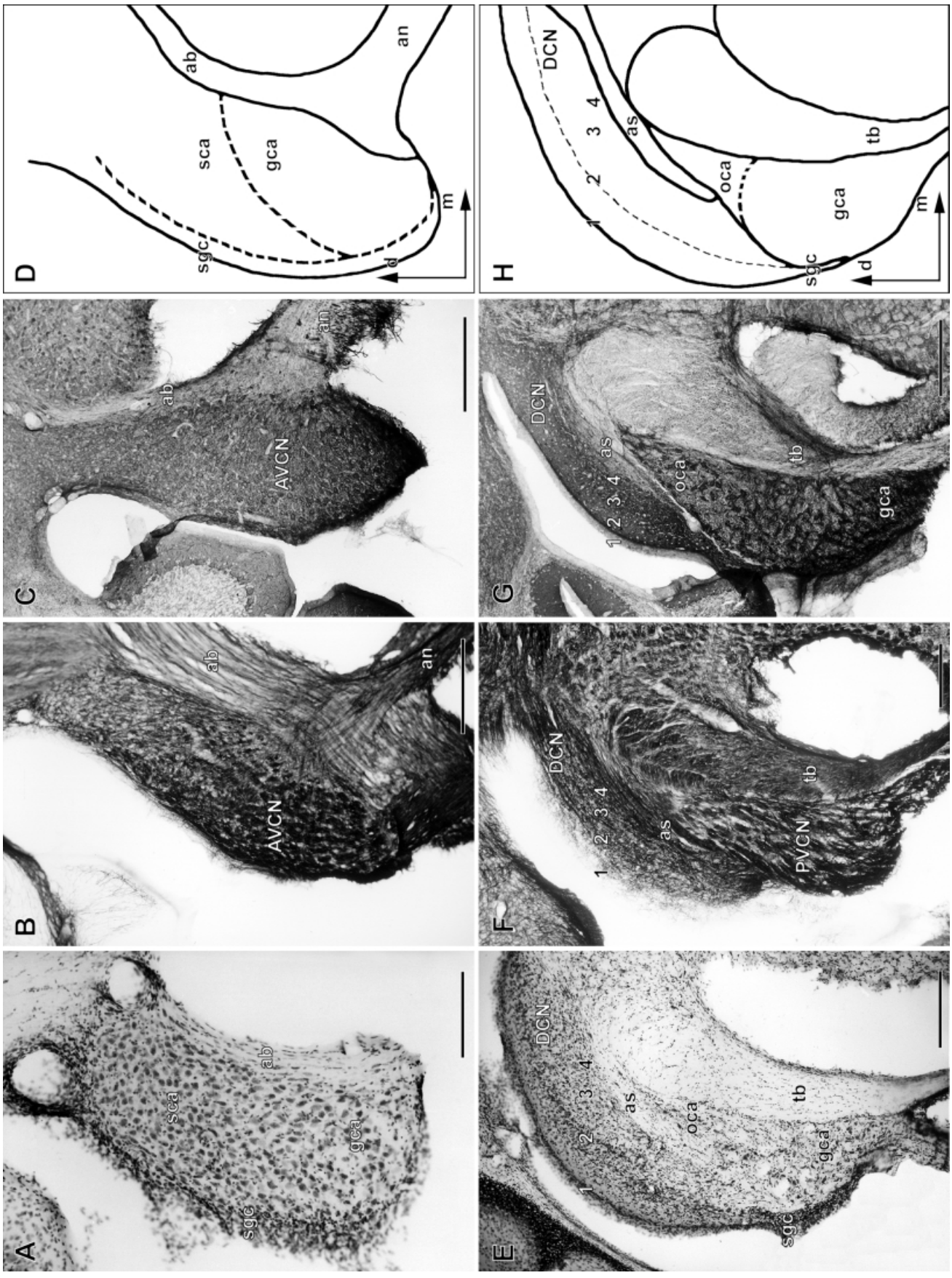
A
sgc
sca
ab
gca
B
AVCN
ab
an
C
AVCN
ab
an
D
sgc
sca
gca
ab
an
d
m
E
DCN
1
2
3
4
as
oca
tb
sgc
gca
F
DCN
1
2
3
4
as
PVCN
tb
G
DCN
1
2
3
4
as
oca
tb
gca
H
DCN
1
2
3
4
as
oca
tb
sgc
gca
d
m

where they also formed terminations. The IC was the only subcortical structure bilaterally labelled. Fibres to the NLL probably originated from the corticocollicular branch.

Because biocytin is transported not only in anterograde but also in retrograde direction (for review see McDonald, 1992) it turned out to be useful for the identification of several subcortical inputs to the auditory cortex. We found a particularly high number of Golgi-like stained cells of origin in the subdivisions of the MGB (Figs 5B and C, and 6D and E, see also Table 1).

Injection sites

The injection foci in the auditory cortex had an average diameter of $390 \pm 90\,\mu m$ and always covered several cortical layers, mostly layers III–V. The injections were targeted at AI, AAF, DP and VP using stereotaxic coordinates and features of the surface vasculature (Fig. 1; see also companion paper Budinger *et al*., 2000). *Post hoc*, after histological preparation, their positions with respect to the auditory cortical fields were microscopically confirmed using the rostral tip of the hippocampus and the dorsal roof of the CPu as internal references (for details see Budinger *et al*., 2000). The hippocampal reference also served to evaluate the positions of the injection sites with respect to the low- and high-frequency representation areas in AI. In previous 2-deoxyglucose studies (Scheich *et al*., 1993) it was shown that along the rostrocaudal dimension the rostral tip of the hippocampus approximately corresponds to the 1 kHz representation in AI. Thus, biocytin injections caudal to this reference were made most probably into low-frequency areas of AI whilst injections rostral to this reference were made into high-frequency areas of AI (see also Fig. 5D–F).

Connections of AI

The strongest subcortical projections from AI are to the MGB. Here, we found many labelled axons and terminations (boutons 'en passant' and 'terminaux') in all subdivisions of the MGB, but most in the MGv (Fig. 6A). Retrogradely filled neurons were found in the MGd and MGm but most in the MGv.

In order to estimate the relative weights of projections from the subdivisions of MGB to AI we counted the number of retrogradely labelled neurons within its major subdivisions in frontal sections after injections of biocytin into AI. As shown in Table 1 most retrogradely labelled neurons were found in the MGv followed by the MGd and MGm. When the injection sites were at more caudal positions within AI, i.e. closer to DP and VP, the number of retrogradely filled neurons was slightly smaller in MGv and larger in MGd than when injections were at more rostral positions within AI.

The large spatial overlap of anterogradely labelled axonal elements and retrogradely filled somata indicates a certain degree of reciprocity in the connections between AI and auditory thalamus. A shift of the injection sites in AI from caudal to rostral with respect to the hippocampal reference, i.e. from low- to high-frequency areas, resulted in a shift of anterograde and retrograde label from laterorostral to mediocaudal in the MGv (Fig. 5D–F). This suggests preferential reciprocal connections between low-frequency areas in AI and laterorostral portions of MGv, between middle-frequency areas in AI and middle portions of MGv, and between high-frequency areas in AI and mediocaudal portions of MGv.

Other nuclei of the thalamus with projections from AI are the SG, the PLi (Fig. 7A and B), the laterodorsal (LD) and lateral posterior (LP) thalamic nucleus, the Rt and SubG. In the SG, PLi, LD and LP, we found diffusely distributed axons with both types of terminals. In the ventroposterior region of Rt, labelled axons formed a small patch of terminations (Fig. 8A and B). In addition, further caudoventrally we detected in all cases projections to the SubG (Fig. 8C and D). The terminations in the Rt and in the SubG appeared as small boutons 'en passant' and 'terminaux'.

We also found projections from AI to the basal ganglia. Axon terminations were seen in the rostromedial and particularly in the caudal parts of the CPu, and in the caudomedial GP (Fig. 9A and C). The amygdalostriatal transition area (AStr), the lateral amygdaloid nucleus (LA) and the basolateral amygdaloid nucleus (BL) also received input from AI (Fig. 9A) but not the central amygdaloid nucleus (CA). The majority of corticoamygdaloid axons terminated in the LA. Terminations in the amygdaloid complex and corpus striatum formed boutons 'en passant' and 'terminaux'.

There were also projections from AI to the colliculi. In the SC, labelled corticocollicular fibres terminated chiefly in deep and intermediate layers but, more sparsely and diffusely distributed, also in other layers (not shown). In the IC, labelled fibres terminated particularly densely in the DCIC and ECIC (Fig. 10A). Only few terminations were found in the CIC. The IC was the only bilaterally labelled subcortical structure, i.e. both the ipsilateral and contralateral IC received direct input from AI of one hemisphere. After passing the commissure of the IC, axons terminated within the contralateral DCIC and ECIC. The ipsilateral and contralateral terminals appeared as boutons 'en passant' and 'terminaux' (Fig. 10B).

Projections to the metencephalon were restricted to the pontine nuclei (Fig. 11H), specifically the dorsolateral pontine area. Here we observed both kinds of synaptic contacts but mainly boutons 'en passant' (Fig. 11I and J).

Connections of AAF

Following injections of biocytin into AAF, labelled axons generally took the same corticofugal pathways as axons labelled following injections into AI. Thus, a main fibre bundle terminated within the auditory thalamus, indicating strong connections of field AAF with the MGB complex, although these were much weaker than those of AI. Within the MGB most anterograde labelling was found in the MGm (Fig. 6C), whereas similar numbers of retrogradely filled neurons (Fig. 6D and E) were counted in the MGm and MGv (Table 1). Again, a high degree of spatial overlap between terminal labelling and retrogradely filled neurons could be observed.

Other labelled corticothalamic fibres were found in the SG, PLi, LP, LD, SubG and Rt. Projections from AAF to the SubG were not as strong as those from AI and the posterior fields. The projections from AAF to the CPu, GP and amygdaloid complex were similar in number and distribution patterns to those from AI. Axon terminations

FIG. 4. Frontal sections showing the cyto-, myelo- and chemoarchitecture of the cochlear nuclei (CN). Orientation in D and H. (A–C) Nissl stain (A), myelin stain (B) and immunoreactivity against parvalbumin (C) of the AVCN. In the Nissl stain, a globular (gca) and a spherical cell area (sgc) and the superficial granule cell layer (sgc) can be identified. The ascending branch (ab) of the auditory nerve (an) innervates the AVCN. (D) Schematic drawing illustrating major outlines of the AVCN. (E–G) Nissl stain (E), myelin stain (F) and immunoreactivity against parvalbumin (G) of the PVCN and DCN. Within the PVCN, a globular (gca) and an octopus cell area (oca) can be identified. Within the DCN four layers (1–4) are distinctive. The fibre tracts of the trapezoid body (tb) and acoustic stria (as) delineate the borders of the CN subdivisions. (H) Schematic drawing illustrating major outlines of the PVCN and DCN. Scale bars, 300 μm.

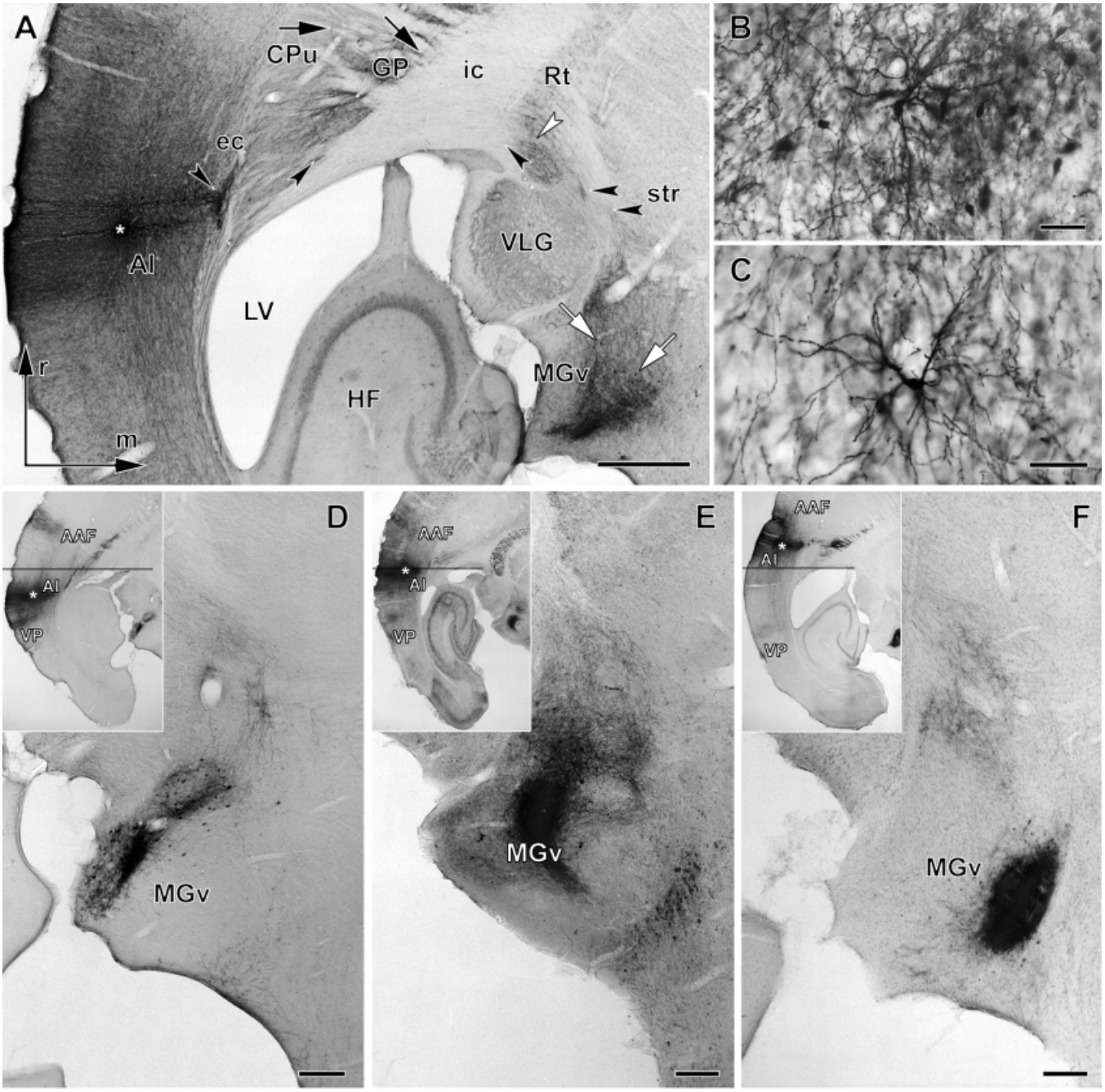

FIG. 5. Labelling patterns after injections of biocytin into the primary auditory field (AI). The injection sites are marked with asterisks. Orientation in A. Methylgreen counterstainings, except in E. (A) Labelled axons after a relatively large injection are visible leaving the auditory cortex and passing the external capsule, internal capsule and superior thalamic radiation (ec, ic and str, all black arrowheads) to terminate in the ventral part of the medial geniculate body (MGv). Axons to the caudate putamen and globus pallidus (CPu and GP, both black arrows) and to the reticular thalamic nucleus (Rt, white arrowhead) are also seen. Anterogradely labelled terminals are clearly visible by dense staining, e.g. in the MGv, where some of the retrogradely labelled cells are indicated by white arrows. (B and C) Single Golgi-like retrogradely labelled neurons in the MGv. (D–F) Systematic shift of anterograde and retrograde labelling in MGv from laterorostral to mediocaudal with a shift of the injection site in AI from caudal (low-frequency area; D) to rostral (high-frequency area; F). The relative location of the injection site in AI was determined with respect to the rostral pole of the hippocampus (horizontal lines in the insets). Parvalbumin counterstaining in E. Scale bars, 300 μm (A), 50 μm (B and C), 200 μm (D–F).

FIG. 6. Anterograde and retrograde transport of biocytin to the medial geniculate body (MGB). Orientation in B. (A) Following an injection into the primary auditory field (AI) anterogradely labelled terminals (e.g. white arrowheads) and retrogradely filled cells of origin (e.g. black arrows) can be found, particularly in the ventral division of the medial geniculate body (MGv). The other subdivisions of the medial geniculate body (MGB) also receive input from and project to the primary auditory field (AI) [white arrows mark retrogradely labelled neurons in dorsal MGB (MGd)]. Note the spatial overlap between anterogradely and retrogradely labelled neuronal elements. Parvalbumin counterstaining. (B) Following an injection into the dorsoposterior auditory field (DP), labelled axons and cell bodies (arrows) are detectable particularly in MGd, but also in the other subdivisions. Methylgreen counterstaining. (C) Following an injection into the anterior auditory field (AAF) the majority of labelled neuronal elements are found in the medial MGB (MGm). Arrows indicate the location of retrogradely filled neurons. Nissl staining. (D and E) Enlarged images of Golgi-like retrogradely labelled cells in the MGm from C. Scale bars, 200 μm (A–C), 50 μm (D and E).

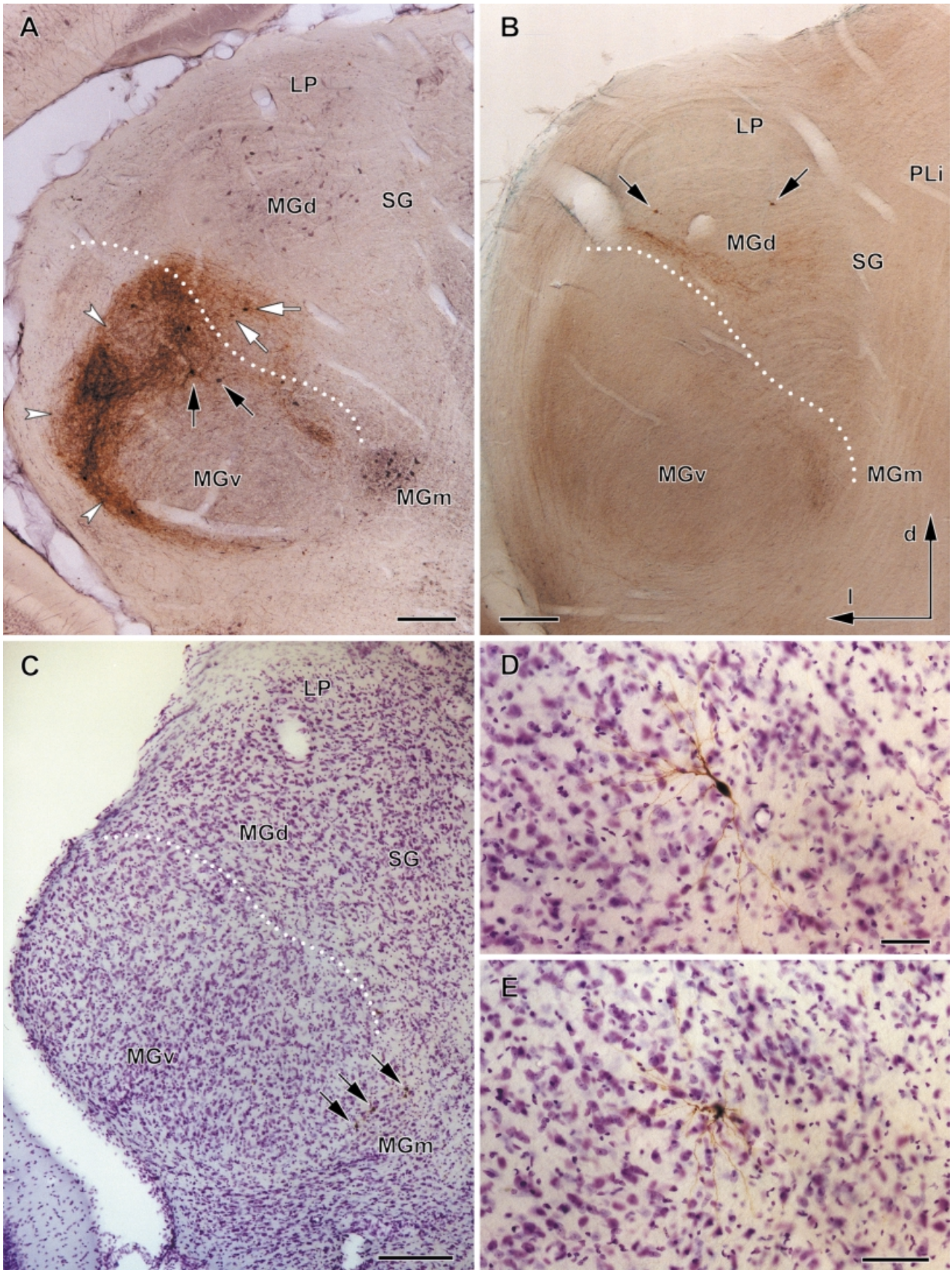
A
LP
MGd
SG
MGv
MGm
B
LP
PLi
MGd
SG
MGv
MGm
d
l
C
LP
MGd
SG
MGv
MGm
D
E

within the amygdala (boutons 'en passant' and 'terminaux') were distributed within the AStr, LA and BL.

Corticocollicular projections from AAF terminated in the ipsilateral DCIC, ECIC and sparsely in the CIC, as well as in the contralateral DCIC and ECIC. Diffusely distributed terminals within the ipsilateral SC were found mainly in the deep and intermediate layers.

In contrast to AI injections single labelled axons were also seen ventral to the IC in the paralemniscal regions around the DNLL and within the DNLL itself (not shown). Terminations were mainly found dorsal and medial to the DNLL, but also within this nucleus. The corticolemniscal axons appeared to stem from the corticocollicular branch. In addition, we found projections from AAF to the SOC (Fig. 11E). The corticoolivary projections took the same trajectory as the corticopontine fibres originating from AAF. Traversing the cerebral peduncle these fibres reached the rostral pole of the SOC and turned ventrally towards an area which probably corresponds to the ventral MVPO and rostral VNTB. Here they formed diverse synaptic contacts (Fig. 11F and G). More caudally the remaining axons terminated within the trapezoid body and could not be traced further. Thus, we found no projections to the CN.

Connections of DP and VP

The subcortical auditory projections of the two posterior auditory fields, DP and VP, appeared similar. The strongest projections from DP and VP were also to the MGB complex. Within the MGB most anterograde labelling was found in the MGd (Fig. 6B) and about the same numbers of retrogradely filled neurons were counted in the MGd and MGv (Table 1). Again, a high degree of spatial overlap between anterogradely and retrogradely labelled structures was observed in the three major subnuclei of the MGB.

Other thalamic structures receiving descending projections from DP and VP were the SG (Fig. 7C and D), PLi, LD, LP (Fig. 7E and F), Rt and SubG. Projections from DP and VP to the SG, PLi, LD and LP were slightly stronger than those from AI and AAF. In addition, we always detected projections, though few, from DP and VP to the dorsal lateral geniculate nucleus (DLG) where axons showed boutons 'en passant' and 'terminaux' (Fig. 12). In one case some of these labelled axons traversed further ventrally towards the ventral lateral geniculate nucleus (VLG).

The corticostriatal projections as well as the corticoamygdaloid projections from DP and VP were similar to the corresponding projections from AI and AAF (Fig. 9B). Again, labelled terminations were found in the CPu, GP, AStr, LA (Fig. 9D) and BL.

The labelled corticocollicular fibres formed terminations in the ipsilateral SC (Fig. 10D and E), in the ipsilateral IC (DCIC, ECIC, CIC) and in the contralateral IC (DCIC, ECIC; Fig. 10C). The projections to the SC reached all layers, but mainly the deep and intermediate layers, and appeared stronger than those originating from AI or AAF.

Sparse corticolemniscal terminations (boutons 'en passant' and 'terminaux') were found around the DNLL and, even sparser, within the DNLL (Fig. 11A–D). The corticoolivary projections terminated in the rostroventral SOC and trapezoid body. Although sparse in number and distribution, the projections from DP and VP to the NLL and SOC were still slightly stronger than those from AAF. The corticopontine projections from DP and VP terminated particularly in the dorsolateral pontine area.

Discussion

Anatomy of auditory subcortical structures

The first aim of the present study was to characterize histologically those subcortical structures of the brain of the Mongolian gerbil which are targets of direct projections from, or provide direct input to, the auditory cortex, with an emphasis on structures of the auditory pathway. We also included the CN (even though we found no biocytin label there) because direct projections from the auditory cortex to the CN have been demonstrated by means of the anterograde transport of *Phaseolus vulgaris*-leucoagglutinin and of the retrograde transport of Fast Blue in the rat (Feliciano *et al*., 1995; Weedman & Ryugo, 1996).

The auditory thalamus

The MGB is the most prominent thalamic auditory nucleus, which has been extensively described in cat (e.g. Winer, 1985), monkey (e.g. Oliver & Hall, 1978a; Pandya *et al*., 1994; Molinari *et al*., 1995; Hackett *et al*., 1998), rat (e.g. Clerici & Coleman, 1990; Winer *et al*., 1999a) and rabbit (e.g. de Venecia *et al*., 1998), and which is commonly divided into ventral, dorsal and medial subdivisions, although further parcellations have been suggested and the nomenclature varies (for review see Winer, 1992). In addition to the MGB, several other auditory thalamic nuclei, such as the SG and Pli, exist (for review see Winer, 1992). In the Mongolian gerbil, the cyto-, myelo- and chemoarchitectural staining patterns (Fig. 2A–D) support this tripartite division of the MGB complex with the SG and PLi bordering the MGB medially. Likewise, the strong immunoreactivity against the calcium-binding protein PV (Celio & Heizmann, 1981) is similar to that described in rabbit (McMullen *et al*., 1994; de Venecia *et al*., 1995, 1998), rat (Celio, 1990) and macaques (Hashikawa *et al*., 1991; Molinari *et al*., 1995), but differs markedly from that previously described for the gerbil (Braun & Piepenstock, 1993). The latter authors reported that the MGB showed no distinct PV immunoreactivity, a discrepancy which may be due to different PV antibodies used in that and in the present study.

It has been suggested that PV is specifically expressed in reciprocal circuits linking the MGB with the IC (Hashikawa *et al*., 1991; de

TABLE 1. Retrogradely labelled neurons in the medial geniculate body (ventral, dorsal and medial divisions) after biocytin injection into the auditory cortex

	Injection in AI ($n = 6$)		Injection in AAF ($n = 4$)		Injection in DP/VP ($n = 4$)	
	N	(%)	*N*	(%)	*N*	(%)
Labelled neurons						
in MGv	140.0 ± 40.4	(75.7 ± 11.9)	9.0 ± 6.5	(41.2 ± 23.1)	41.2 ± 37.5	(42.3 ± 28.3)
in MGd	43.0 ± 33.6	(22.0 ± 12.8)	2.0 ± 0.8	(11.9 ± 9.2)	45.8 ± 22.9	(54.9 ± 30.1)
in MGm	4.8 ± 6.1	(2.3 ± 2.8)	9.3 ± 4.8	(46.9 ± 20.2)	2.5 ± 1.9	(2.8 ± 2.0)
Totals	187.8 ± 58.0	(100)	20.3 ± 6.8	(100)	89.5 ± 43.6	(100)

n, number of animals; *N*, number of cells. Values are averaged numbers and, in brackets, proportions of labelled neurons, mean ± 1 SD.

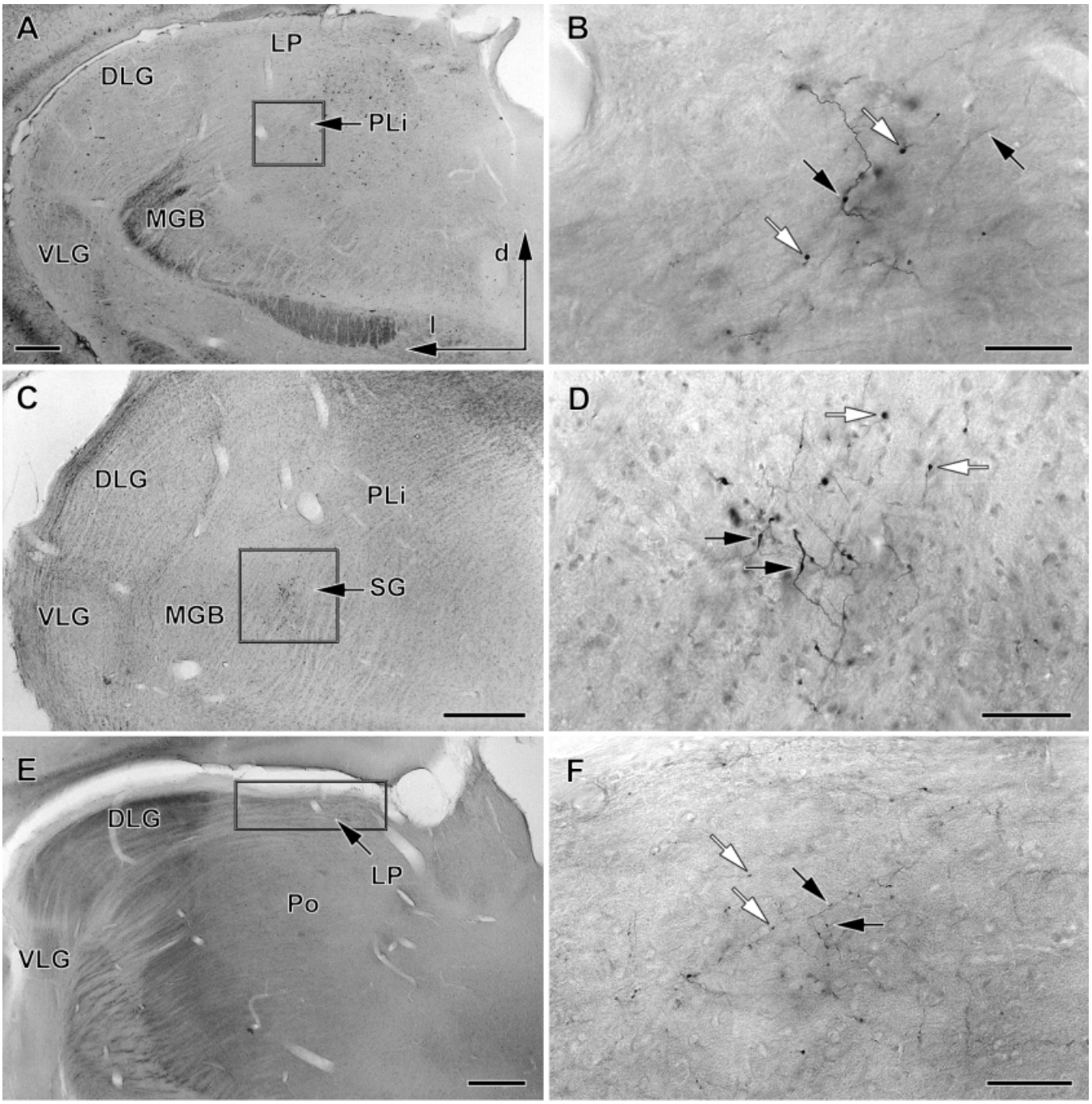

FIG. 7. Anterograde transport of biocytin to the thalamus. Orientation in A. (C–F) Methylgreen counterstaining, (A and B) parvalbumin counterstaining. (A, C and E) Labelled axons in the posterior limitans nucleus (PLi, arrow in A) following an injection into the primary auditory field (AI), in the suprageniculate nucleus (SG, arrow in C) following an injection into the ventroposterior auditory field (VP), and in the lateroposterior thalamic nucleus (LP, arrow in D) following an injection into the dorsoposterior auditory field (DP). (B, D and F) Enlarged photographs of framed areas in A, C and E, respectively, showing boutons 'en passant' (black arrows) and 'terminaux' (white arrows) in the PLi, SG and LP, respectively. Scale bars, 400 μm (A, C and E) and 50 μm (B, D and F).

Venecia *et al*., 1995) and the auditory cortex (Hashikawa *et al*., 1991, 1995; McMullen *et al*., 1994; Molinari *et al*., 1995; de Venecia *et al*., 1998). In the present study, connections between the IC and the MGB were not investigated, but a strong pathway from the CIC to the MGv is likely to exist in the gerbil as it does in all other mammals studied (for review see Oliver & Huerta, 1992; Winer, 1992). Because the CIC is strongly PV-positive and contains the majority of PV-positive somata (Fig. 2G), these PV-positive neurons could project to the MGv and account for the high concentration of PV-positive axonal terminations there. A relationship of the differential PV immunoreactivity of MGB subdivisions with that of the auditory cortical fields in the gerbil is also indicated. We have shown in the companion paper (Budinger *et al*., 2000) that the PV immunoreactivity of neuronal elements in the auditory cortex is most pronounced in the thalamocortical input and corticothalamic output layers of the two core fields AI and AAF. Because AI and AAF are predominantly and reciprocally connected with the MGv and MGm, respectively (Table 1), which both show the highest PV concentration of the

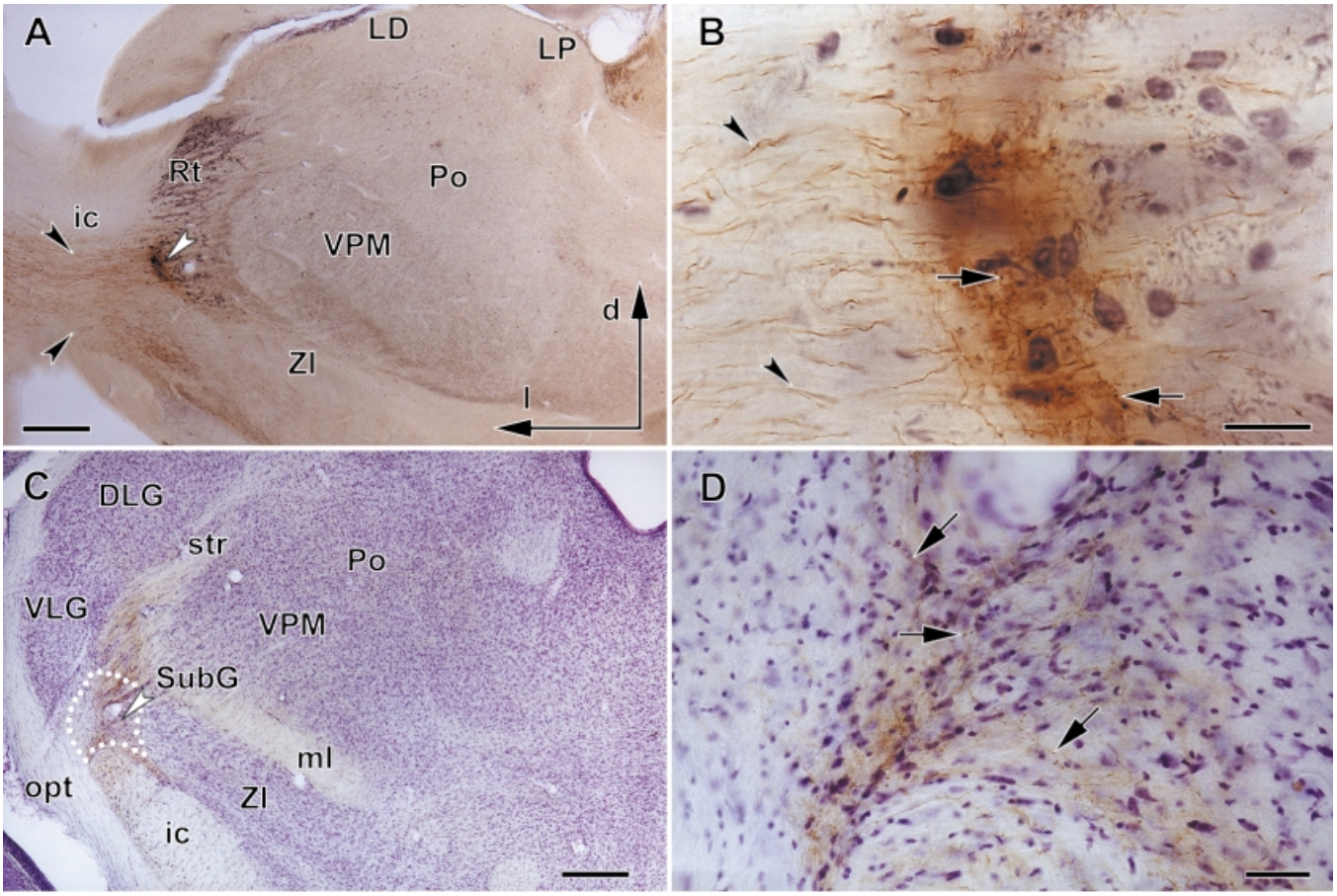

FIG. 8. Anterograde transport of biocytin to the thalamus following injections into the primary auditory field (AI). Orientation in A. (A) Labelled axons, traversing the internal capsule (ic) and entering the thalamus (black arrowheads), form a patch in the ventrocaudal region of the reticular thalamic nucleus (Rt, white arrowhead; enlarged in B). Parvalbumin counterstaining. (B) Enlarged photograph from A showing traversing axons (e.g. arrowheads) as well as various boutons (e.g. arrows) in the Rt. (C) Further caudoventrally there is another focus of labelled axons in the subgeniculate thalamic nucleus (SubG, arrowhead; enlarged in D). Nissl staining. (D) Enlarged photograph from C showing densely distributed axons and terminals (e.g. arrows) in the SubG. Scale bars, 400 µm (A and C), 50 µm (B and D).

MGB subdivisions, the existence of a specific circuit between the auditory cortex and the MGB, related to the strength of PV immunoreactivity, seems possible in the gerbil.

The auditory structures of the mes- and metencephalon

The IC has been investigated anatomically in various mammalian species with most detailed studies in cat, where, based on Golgi preparations, a tripartite central nucleus, a bipartite cortex and several paracentral nuclei and pericollicular areas were recognized (for review see Morest & Oliver, 1984; Oliver & Huerta, 1992). In the gerbil, the staining methods for cell bodies, myelinated fibres and PV allowed the identification of three main subdivisions of the IC (Fig. 2E–H), namely a large central nucleus (CIC), a dorsal cortex (DCIC) and an external cortex (ECIC). This parcellation corresponds to that of the rat IC (Faye-Lund & Osen, 1985; Coleman & Clerici, 1987; Herbert *et al.*, 1991). A further detailed parcellation of the gerbil's IC and surrounding areas as in the cat (e.g. Morest & Oliver, 1984) was not possible without Golgi-impregnated material.

The NLL of the gerbil can be subdivided into a dorsal (DNLL), intermediate (INLL) and bipartite ventral nucleus (dVNLL, vVNLL). The DNLL, INLL and vVNLL form three distinct oval nuclei interspersed with the thick fibre tracts of the LL (Fig. 3A–D). In sections stained for PV, the subdivisions of the gerbil's NLL can be clearly recognized and a variety of cells can be identified. It has been proposed that the intense PV staining of neurons in the auditory brainstem is correlated with their high metabolic rate and thus with a great potential capacity for oxidative metabolism and rapid transmission (e.g. Seto-Ohshima *et al.*, 1994; Caicedo *et al.*, 1996).

As shown in the present study the subnuclei of the gerbil's SOC are generally well distinguishable based on architectonic features and relative location (Fig. 3E–H). Cells of various size and shape (for comparison see Schwartz, 1992), most of them PV-immunopositive, form more-or-less compact aggregates encircled by thick myelinated fibre tracts allowing the distinction of 12 subnuclei. We suggest that the SOC of the gerbil consists of a lateral (LSO) and medial superior olivary nucleus (MSO), a medial (MNTB), ventral (VNTB) and lateral nucleus of the trapezoid body (LNTB), and seven periolivary nuclei (SPN, MVPO, LVPO, DPO, DLPO, RPO, CPO). In other species, the SOC has been subdivided into up to 13 distinct nuclei (for review see: rat, Harrison & Feldmann, 1970; guinea pig, Schofield & Cant, 1991; cat, Schwartz, 1992).

Although various domains of different cell types form the CN in the gerbil, three major subdivisions are characteristic for this auditory structure (Fig. 4): two compact ventral nuclei (AVCN and PVCN), each consisting of at least two separate cell areas, and a laminated dorsal nucleus (DCN). This finding is in general accordance with

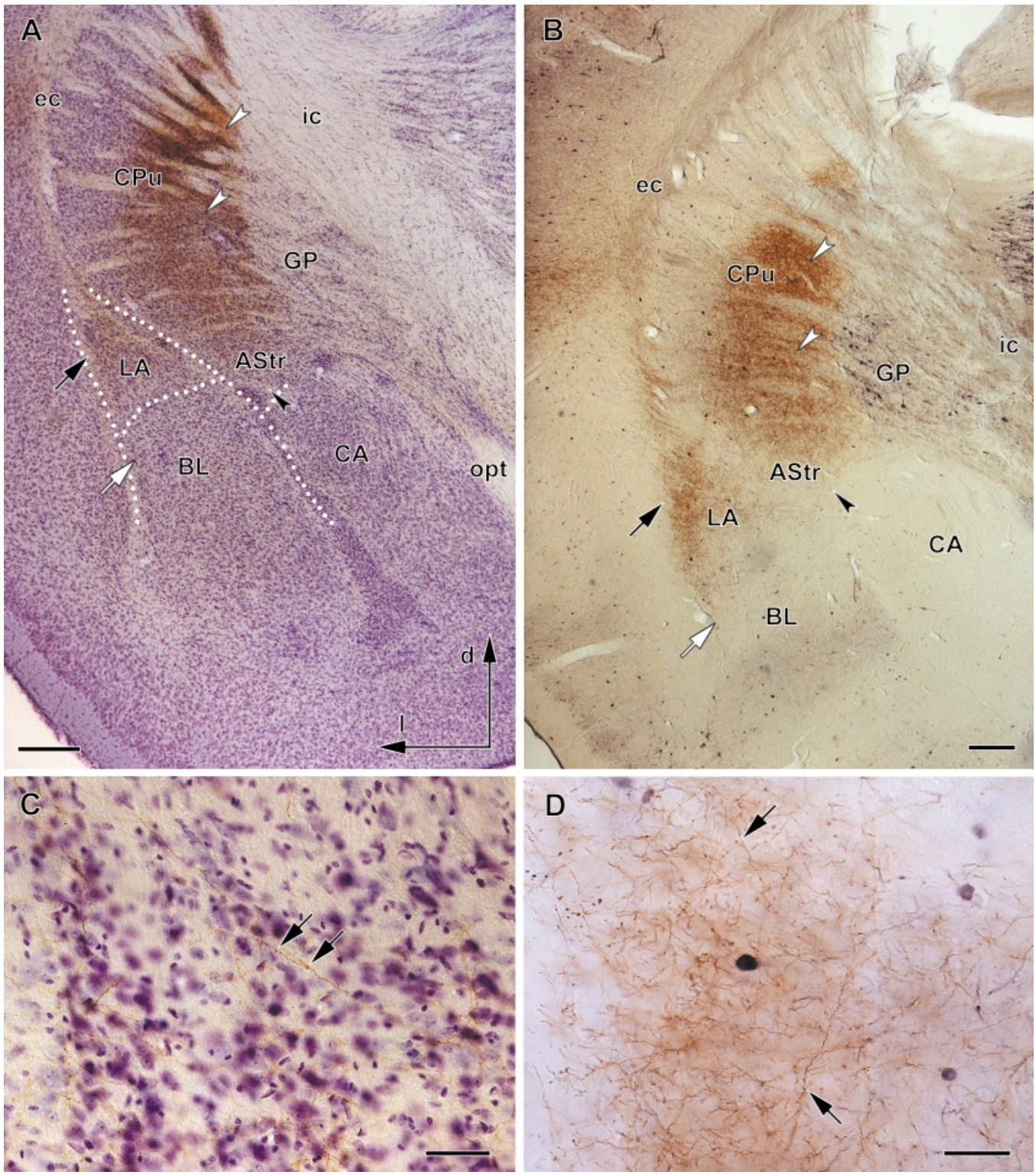

FIG. 9. Anterograde transport of biocytin to the striatum and amygdaloid complex. Orientation in A. (A) Labelled axons in the caudate putamen (CPu, white arrowheads), globus pallidus (GP), amygdalostriatal transition area (AStr, black arrowhead), lateral amygdaloid nucleus (LA, black arrow) and basolateral amygdaloid nucleus (BL, white arrow) following an injection into the primary auditory field (AI). Nissl staining. (B) Labelled axons in the CPu (white arrowheads), GP, AStr (black arrowhead), LA (black arrow) and BL (white arrow) following an injection into the dorsoposterior auditory field (DP). Note that there is no labelling in the central amygdaloid nucleus (CA). Parvalbumin counterstaining. (C) Enlarged photograph from A showing labelled axons and terminations (arrows) in the GP. (D) Enlarged photograph from B showing labelled axons and terminations (arrows) in the LA. Labelled cells contain parvalbumin. Scale bars, 200 µm (A and B), 50 µm (C and D).

studies in rat (for review see, e.g., Harrison & Feldmann, 1970), cat (e.g. Osen, 1969; Brawer *et al*., 1974; for review see Cant, 1992) and guinea pig (Hackney *et al*., 1990). Many different cell types of CN neurons (for comparison see Osen, 1969; Brawer *et al*., 1974;

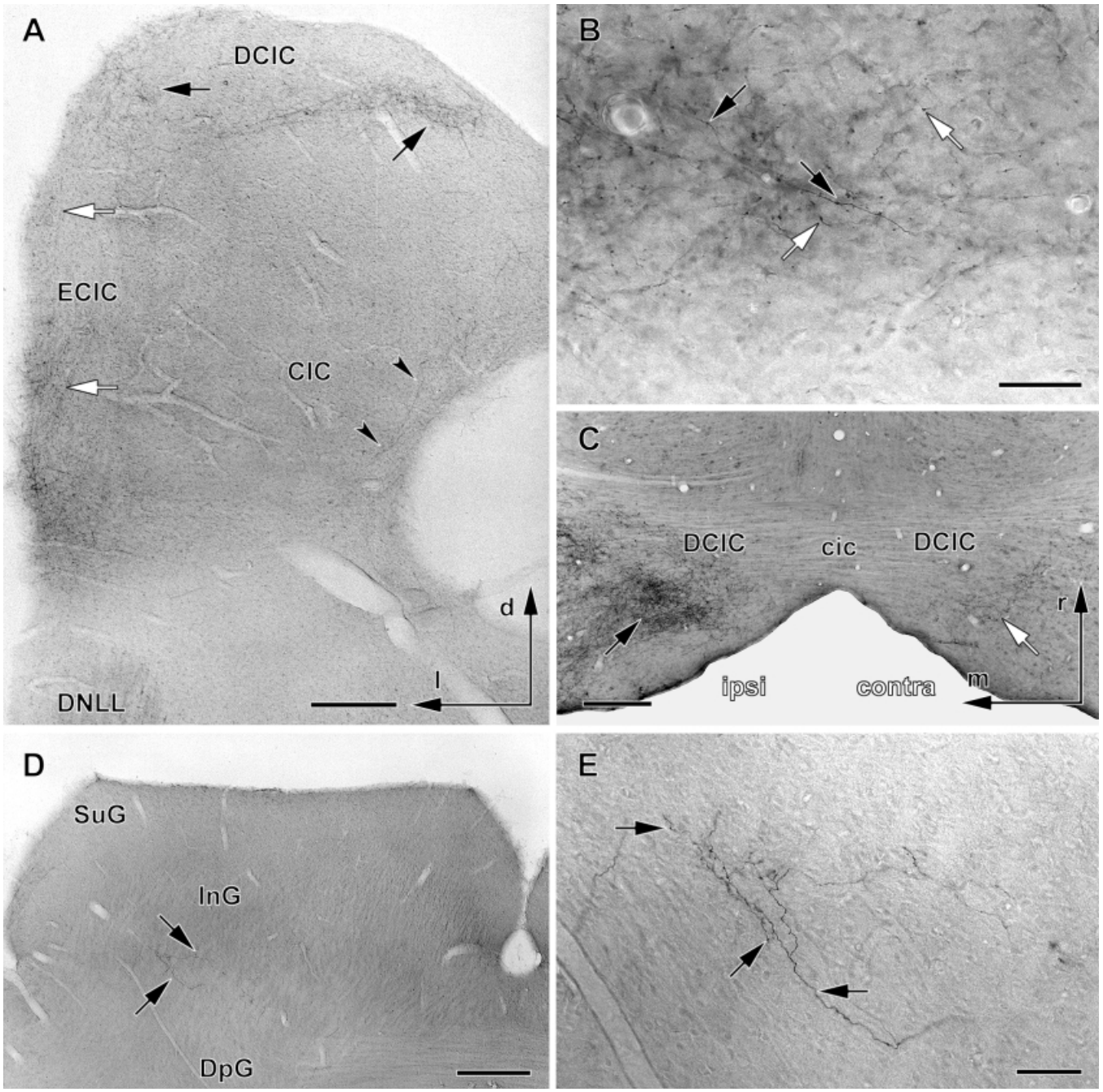

FIG. 10. Anterograde transport of biocytin to the colliculi following injections into the auditory cortex. Orientation in A applies to all panels except C. Methylgreen counterstainings. (A) Projections from the primary auditory field (AI) to the ipsilateral inferior colliculus (IC). Labelled axons can be found particularly in the dorsal cortex (DCIC, black arrows) and in the external cortex (ECIC, white arrows), but also in the central nucleus (CIC, arrowheads) of the IC. (B) Enlarged photograph from A showing boutons 'en passant' (black arrows) and 'terminaux' (white arrows) in the DCIC. (C) Horizontal section showing projections to the ipsilateral (black arrow) and contralateral IC (white arrow) following an injection into the ventroposterior auditory field (VP). Labelled axons cross the midline via the commissure of the IC (cic). (D) Projections to the ipsilateral superior colliculus following an injection into the dorsoposterior auditory field (DP). Labelled axons can be found particularly in the deep (DpG) and intermediate layers (InG). (E) Enlarged photograph from D showing labelled axons and terminations (arrows) in the transition area between DpG and InG. Scale bars, 300 µm (A, C and D), 50 µm (B and E).

FIG. 11. Anterograde transport of biocytin to various brainstem structures. Orientation in A. Nissl stains. (A) Frontal section showing the dorsal nucleus of the lateral lemniscus (DNLL) with microscopically visible projections (arrows, enlarged in B–D) after an injection into the dorsoposterior auditory field (DP). (B–D) Enlarged photographs from A showing labelled axons with boutons 'en passant' (black arrows) and 'terminaux' (white arrows). (E) Direct projections from the anterior auditory field (AAF) to the superior olivary complex (SOC). Labelled axons terminate in the ventral portion of the medioventral periolivary nucleus (MVPO) and rostral portion of the ventral nucleus of the trapezoid body (VNTB) (frame, regions around arrows are enlarged in F and G). (F and G) Enlarged photographs from framed area in E showing boutons 'en passant' (black arrows) and 'terminaux' (white arrows) in the ventral SOC. (H) Direct projections from the auditory cortex to the pontine nuclei following an injection into the primary auditory field (AI). Axons passing the longitudinal fasciculus pons (lfp) enter the dorsolateral pontine area (dlpa, rectangles). (I) Enlarged photograph from upper framed area in H showing labelled axons leaving the lfp to enter the dlpa (arrows). (J) Enlarged photograph from lower framed area in H showing labelled axons ramifying in the dlpa (arrows). Scale bars, 200 µm (A, E and H), 10 µm (B–D), 25 µm (F, G, I and J).

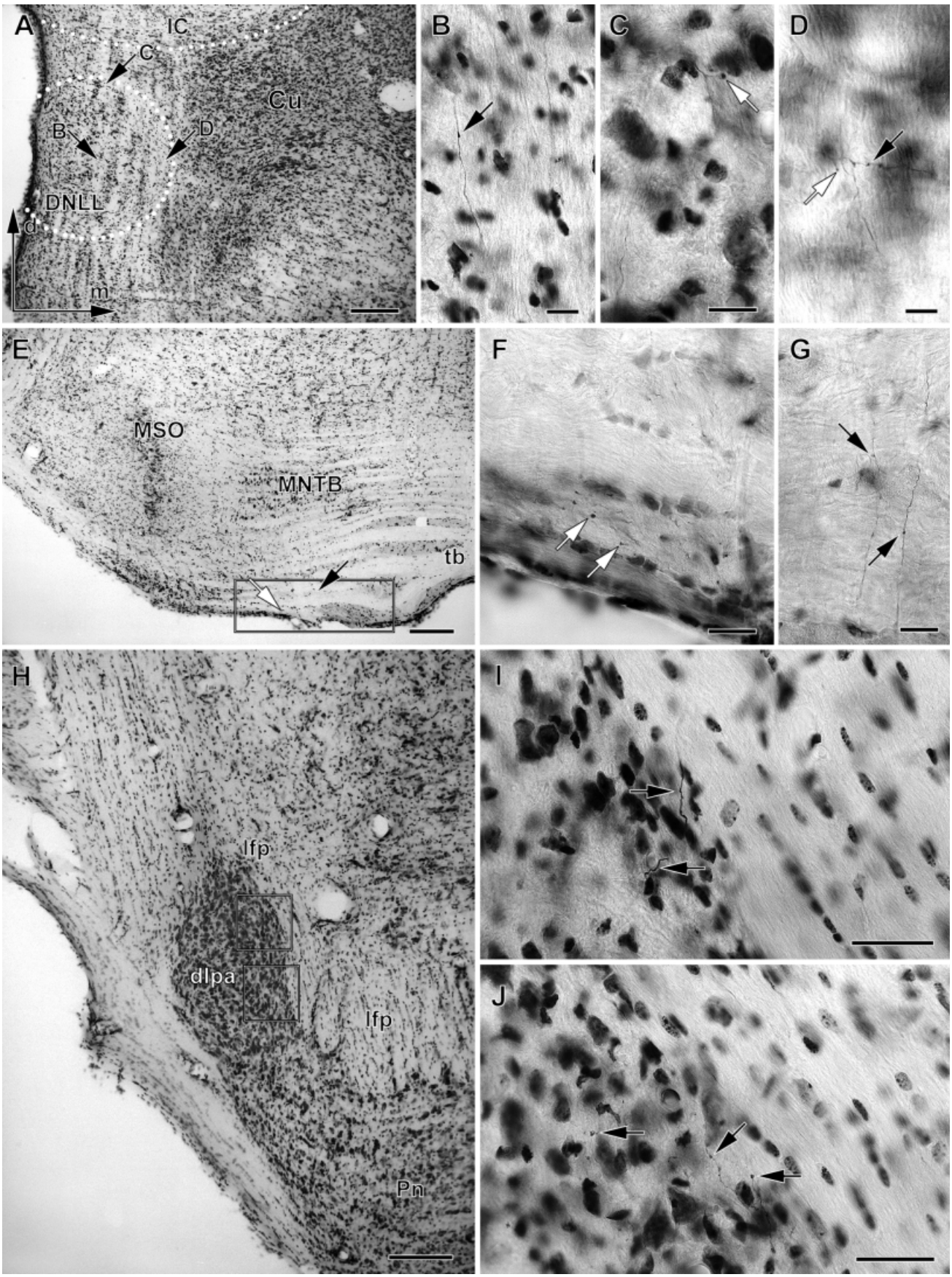
A
IC
C
Cu
B
D
DNLL
d
m
B
C
D
E
MSO
MNTB
tb
F
G
H
lfp
dlpa
lfp
Pn
I
J

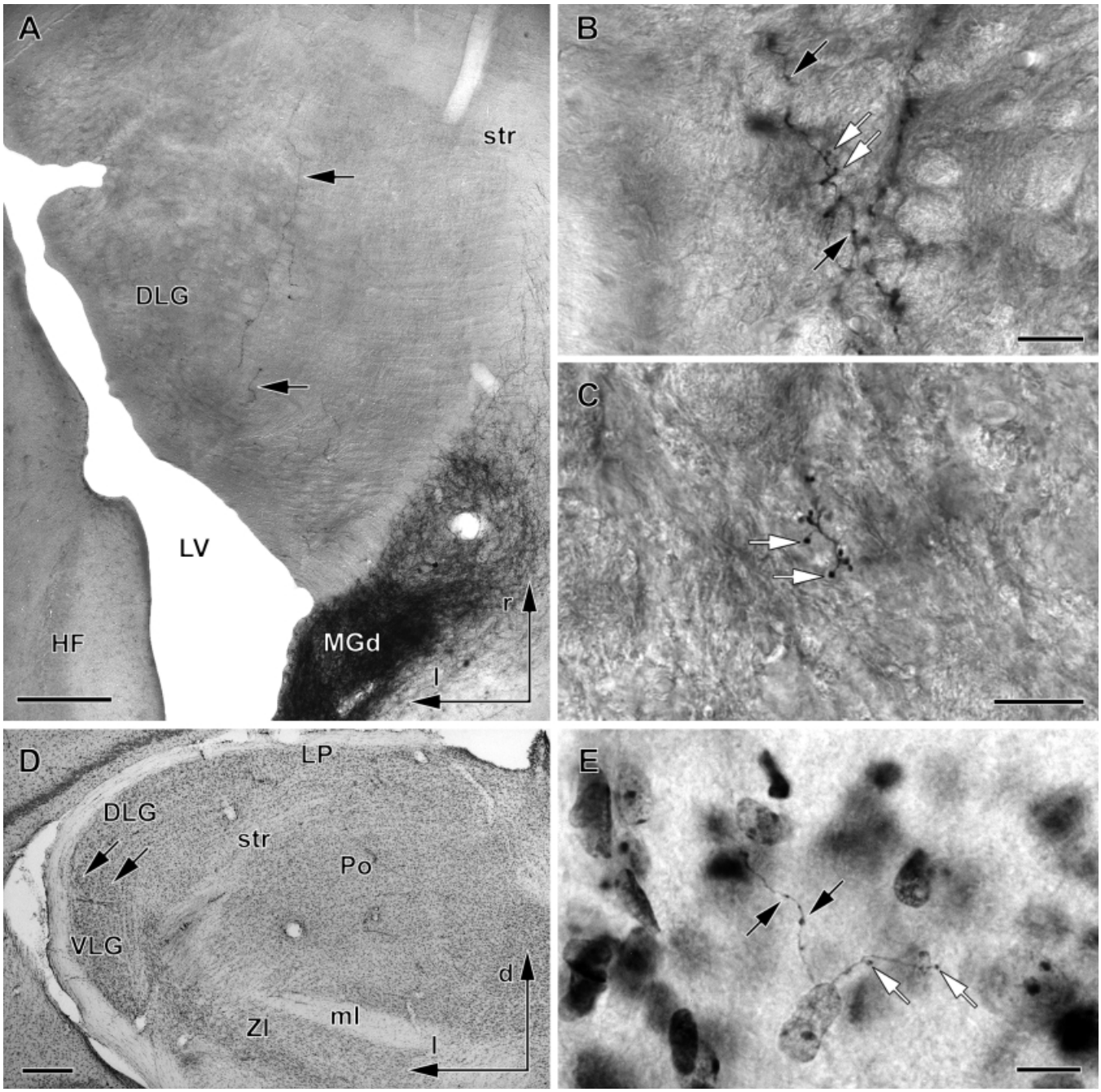

FIG. 12. Anterograde transport of biocytin into the dorsal lateral geniculate nucleus (DLG) after an injections into the dorsoposterior auditory field (DP). (A) Horizontal section with labelled axons in the DLG indicated by arrows. Methylgreen counterstaining. (B and C) Enlarged photographs from A showing boutons 'en passant' (black arrows) and 'terminaux' (white arrows) in the DLG. (D) Frontal section through the thalamus showing location of labelled axons in the ventral DLG (arrows). Nissl staining. (E) Enlarged photograph from D showing boutons 'en passant' (black arrows) and 'terminaux' (white arrows) in the ventral DLG. Scale bars, 200 µm (A), 20 µm (B and C), 500 µm (D), 15 µm (E).

Hackney *et al*., 1990; Lohmann & Friauf, 1996) in the gerbil contain PV.

Subcortical connections of auditory cortex

The second aim of this study was to examine the subcortical connections of the Mongolian gerbil's auditory cortex. This was of particular interest not only because of the increasing importance of this animal for auditory research, but also because only few data are available about the subcortical connections of physiologically defined auditory fields in rodents. These are restricted to connections of the ultrasonic field in mouse (Hofstetter & Ehret, 1992), to thalamocortical connections in the guinea pig (Redies *et al*., 1989) and to thalamic connections of temporal cortex area 1 (Te1) in rat (Winer *et al*., 1999b). Other studies in rat have been related to auditory cortical areas Te1–Te3 as defined by cytoarchitectonic criteria only (e.g. Scheel, 1988; Roger & Arnault, 1989; Arnault & Roger, 1990; Vaudano *et al*., 1991; Mascagni *et al*., 1993; Romanski & LeDoux,

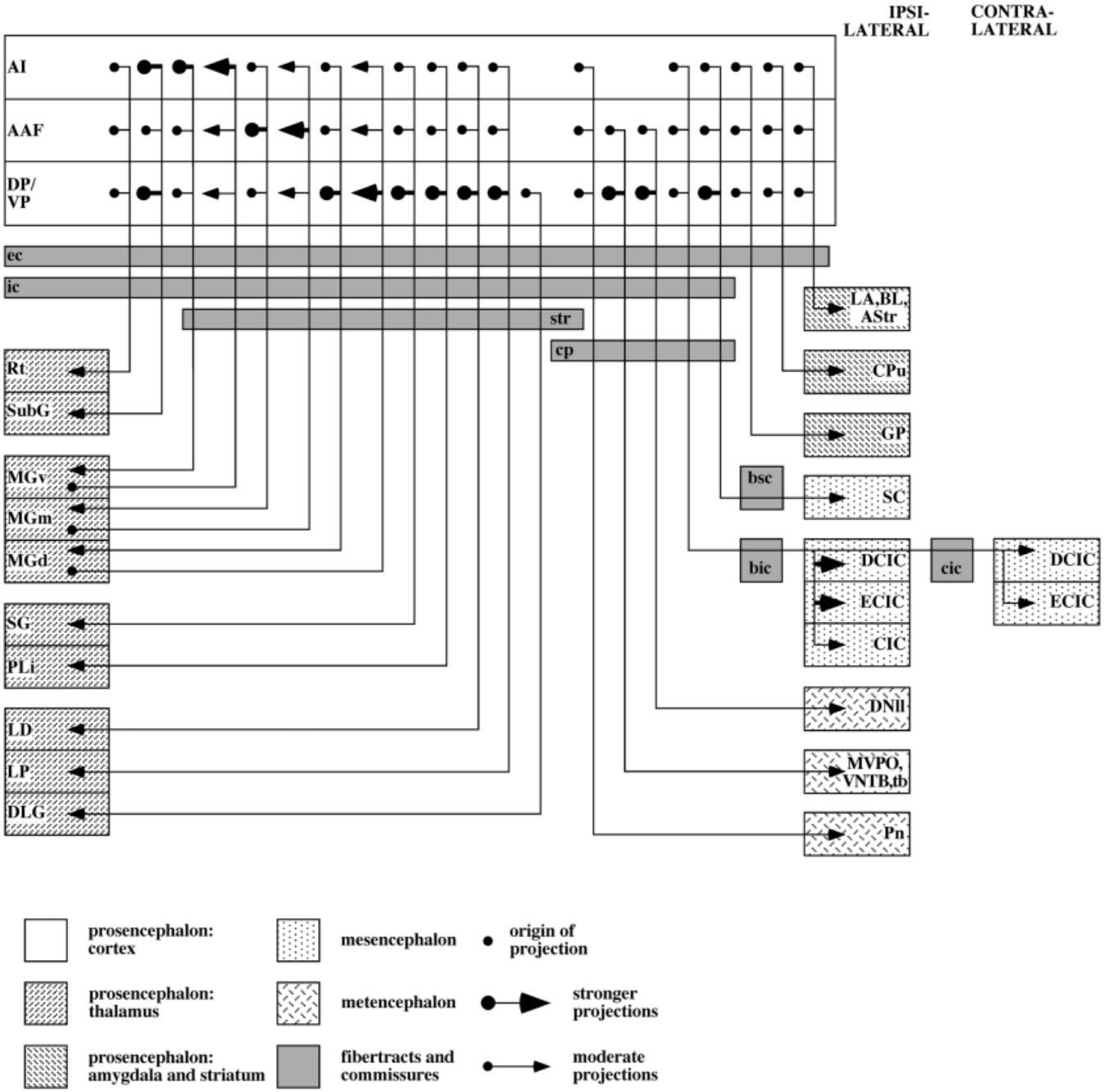

FIG. 13. Summary diagram of the subcortical connections of primary (AI), anterior (AAF) and posterior fields (DP and VP) of the auditory cortex of the Mongolian gerbil as revealed in the present study by anterograde and retrograde transport of biocytin. Additional connections probably exist. The origin of a projection is represented by a filled circle and the target by an arrow. Bold and thin symbols indicate the relative strength of connections within a column, but not within a row.

1993; Shi & Cassell, 1997), but how these in turn relate to physiologically established tonotopic maps (Sally & Kelly, 1988; Horikawa *et al*., 1988) is not entirely clear.

In the present study we focused on the four tonotopically organized auditory cortical fields AI, AAF, DP and VP in the gerbil. Although we did not record physiological properties of neurons at the injections sites, the injected auditory fields and low- and high-frequency areas of AI, respectively, could be identified by stereotaxic coordinates, by internal references and by the comparison of cortical labelling patterns with tone-induced, i.e. frequency-specific, 2-deoxyglucose labelling patterns (for details see companion paper Budinger *et al*., 2000; Scheich *et al*., 1993).

The auditory cortex of the Mongolian gerbil has a variety of subcortical projections to and connections with auditory, visual, multisensory and associational structures in the pros-, mes- and metencephalon, which are summarized in Fig. 13. In all target structures we found both boutons 'en passant' and 'terminaux' in variable but not further analysed proportions. Although the overall projectional patterns are similar for AI, AAF, DP and VP, there are some differences particularly with respect to the strength of

connections suggesting different but overlapping functions of these fields within descending auditory processing.

In the following we will discuss the specific connections of the gerbil's auditory cortex with respect to previous results from other mammals and possible functions.

Projections to structures of the ascending auditory system

Some of the most substantial subcortical projections of the gerbil's auditory cortical fields are to structures of the ascending auditory system, namely the MGB, IC, DNLL and ventral parts of the SOC. These projections differ for AI, AAF, DP and VP, particularly those to the MGB, DNLL and SOC (Fig. 13).

The four tonotopic fields have largely reciprocal connections with all subdivisions of the MGB but the relative strengths of connections differ (Table 1, Fig. 6). The strongest connections of AI are with the MGv, of AAF with the MGm and MGv, and of DP and VP with the MGd and MGv. These results are in general agreement with tracing studies in cat, monkeys and rodents, which have also shown a high degree of reciprocity (e.g. Andersen *et al*., 1980a; Winer & Larue, 1987) and a largely similar topography of corticothalamic and thalamocortical connections (for review see Winer, 1992). The connections between tonotopic parts of the auditory cortex and MGB, particularly MGv, are most probably frequency-specific (e.g. Imig & Morel, 1984; Morel & Imig, 1987; Aitkin *et al*., 1988; Rouiller *et al*., 1989; McMullen & de Venecia, 1993; Winer *et al*., 1999b). In the gerbil we were able to demonstrate, at least for AI, that low-frequency areas are predominantly connected with laterorostral portions of MGv, whereas high-frequency areas are connected with mediocaudal portions of MGv (Fig. 5D–F). It is therefore very likely that in the gerbil's MGv low frequencies are represented laterorostrally, high frequencies mediocaudally and middle frequencies in between. In the cat, detailed descriptions of the frequency representation within MGv are available (e.g. Imig & Morel, 1984; for review see Clarey *et al*., 1992). Here, the low- to high-frequency gradient runs roughly from lateral to medial. In the rat MGv, a similar low- to high-frequency organization from lateral to medial has been suggested based on retrograde tracing of inputs to electrophysiologically identified loci in Te1 (Winer *et al*., 1999b). In contrast, in the guinea pig MGv, the low- to high-frequency gradient runs roughly from caudal to rostral (Redies *et al*., 1989). However, the cortical frequency gradients of the guinea pig's primary areas (fields A, DC) also run in opposite directions to those in the homologous fields of cat, rat and gerbil.

We also found projections from AI, AAF, DP and VP to the ipsilateral and the contralateral IC (Fig. 10A–C), with densest labelling in the ECIC and particularly in the DCIC. Such direct projections from the auditory cortex to the IC bilaterally have been described in detail for many other mammals, but the existence of projections to the CIC is still controversial; some authors mentioned such projections (Diamond *et al*., 1969; Rockel & Jones, 1973a,b; Forbes & Moskowitz, 1974; Fitzpatrick & Imig, 1978; Andersen *et al*., 1980b; Coleman & Clerici, 1987; Luethke *et al*., 1989; Morel & Kaas, 1992; Winer *et al*., 1998) whilst others did not (Oliver & Hall, 1978b; Faye-Lund, 1985; Roger & Arnault, 1989; Arnault & Roger, 1990; Herbert *et al*., 1991; Vaudano *et al*., 1991; Hofstetter & Ehret, 1992). In the gerbil, projections to the ipsilateral CIC clearly exist, but they are weak (Fig. 10A).

We also found sparse projections originating from the anterior and posterior auditory fields, but not from AI, to paralemniscal regions around the DNLL, to this nucleus itself (Fig. 11A–D), and to the rostroventral aspect of the SOC (Fig. 11E–G). Projections to regions within the NLL have also been demonstrated from the ultrasonic field in mouse (Hofstetter & Ehret, 1992) and from Te1 in rat (Feliciano *et al*., 1995) and from the latter structure also to the SOC (Feliciano *et al*., 1995). In the gerbil, labelled axons were also present in the trapezoid body. This finding indicates the possibility of projections from the auditory cortex to auditory structures even more peripheral than the NLL and SOC, i.e. to the CN. Such projections have been demonstrated in the rat by means of the retrograde transport of Fast Blue injected into the CN (Weedman & Ryugo, 1996) or of the anterograde transport of *Phaseolus vulgaris*-leucoagglutinin injected into the cortex (Feliciano *et al*., 1995). This lectin is particularly suited for tracing long-range connections (Gerfen & Sawchenko, 1984) because it is much more stable than, for instance, biocytin (for review see McDonald, 1992). The decomposition of biocytin forces an experimental time limit of about 24 h, and thus it is possible that biocytin may not have reached the CN during this time. It is also possible that for this reason the projections to the DNLL and SOC in the gerbil are much sparser than described for the rat (Feliciano *et al*., 1995).

Projections to other auditory-related thalamic nuclei

In addition to the projections from the auditory cortex to the MGB we found projections to other auditory-related thalamic structures, namely the SG (Fig. 7C and D), PLi (Fig. 7A and B), Rt (Fig. 8A and B) and SubG (Fig. 8C and D). Again, the relative strengths of these projections vary for the different fields (Fig. 13).

Projections from the auditory cortex to SG and PLi are well established in various mammalian species (for review see Winer, 1992). In the Mongolian gerbil, nonprimary posterior auditory fields seem to be more tightly associated with these two thalamic nuclei, as is the case in rat (Scheel, 1988), cat (Winer *et al*., 1977; Mitani *et al*., 1987) and monkeys (Morel & Kaas, 1992; Morel *et al*., 1993; Pandya *et al*., 1994; Rauschecker *et al*., 1997; Hackett *et al*., 1998). The SG and PLi also receive visual input (e.g. Jones & Powell, 1971; Burton & Jones, 1976; Takahashi, 1985; Hicks *et al*., 1986; Katoh & Benedek, 1995). Projections from the auditory cortex to the Rt as well as connections of the Rt with the MGB are substantial in the modulation of auditory processing and have also been demonstrated in different species (Jones, 1975; Rouiller *et al*., 1985; Villa, 1990; Conley *et al*., 1991; Crabtree, 1998). The first evidence for an auditory function of the SubG, which is located ventral to the lateral geniculate complex, was obtained in the gerbil from increased metabolic activity following injection of $GABA_A$ (gamma-amino butyric acid)-receptor antagonists into the auditory cortex (Richter *et al*., 1999). In the present study we showed that this thalamic nucleus also receives direct projections from the auditory cortex.

Projections to structures of the visual pathway

The present study has shown that, in the gerbil, there are also direct projections from the auditory cortex to structures of the visual pathway, in addition to the SG and PLi (see above). We found projections from AI, AAF, DP and VP, but particularly from the posterior fields, to the SC (Fig. 10D and E), LD and LP (Fig. 7E and F) as well as projections to the DLG from DP and VP (Fig. 12).

Auditory cortical projections to the SC have already been demonstrated (e.g. Paula-Barbosa & Sousa-Pinto, 1973; Druga & Syka, 1984; Meredith & Clemo, 1989) and might contribute to the neuronal representation of auditory space in the deeper regions of the SC (for review see Oliver & Huerta, 1992). Projections to the DLG, as found here, have not been reported before. In cat, large lesions of temporal cortex which, however, exceeded the auditory cortex dorsally (case 202; Diamond *et al*., 1969; Jones & Powell, 1971) and ventrally (case 214; Jones & Powell, 1971) resulted in axon and

terminal degeneration and in cell loss in the lateral geniculate nucleus. We showed that, in the gerbil, exclusively posterior auditory fields project to the DLG. The function of connections between the auditory cortex and the DLG are unclear. An increased metabolic activation of the DLG, following acoustic stimulation, has been demonstrated in the blind mole rat (Bronchti *et al*., 1989). Connections between the auditory cortex and the LD and LP have been demonstrated in several species (Diamond *et al*., 1969; Jones & Powell, 1971; Winer *et al*., 1977; Mitani *et al*., 1987; Scheel, 1988; Vaudano *et al*., 1991; Pandya *et al*., 1994; Shi & Cassell, 1997) and are thought to be involved in the relay of sensory, mainly visual, and nonsensory information, because LD and LP have connections with the visual cortex and visual structures of the thalamus and midbrain, as well as with the limbic cortex (e.g. Thompson & Robertson, 1987a,b; Van Groen & Wyss, 1992).

Overall, we showed that the posterior auditory fields in the gerbil have stronger connections than AI and AAF with primary visual (SC and DLG) and visually related subcortical structures (SG, PLi) as well as with the secondary visual cortex (see companion paper Budinger *et al*., 2000).

Projections to the amygdala, basal ganglia and pontine nuclei

We also found projections from the auditory cortex to the amygdaloid complex, which is involved, for example, in the processing of sensory stimuli in relation to behaviour, memory and motivation (for review see, e.g., LeDoux, 1992; McDonald, 1998). In the gerbil, projections from AI, AAF, DP and VP to the AStr, LA and BL have been established, but not to the CA (Fig. 9A, B and D). Projections from auditory cortical areas, except from the primary area, to the amygdala have been demonstrated in the rat (Vaudano *et al*., 1991; Mascagni *et al*., 1993; Romanski & LeDoux, 1993; Shi & Cassell, 1997), cat (Reale & Imig, 1983) and in monkeys (for review see Amaral *et al*., 1992; McDonald, 1998). It has been proposed more generally that the amygdala does receive direct input from higher-level areas only, but not from primary sensory areas, except from the olfactory cortex (for review see Amaral *et al*., 1992; McDonald, 1998). Our data, as well as recent results from the cat (Moreu *et al*., 1999), which show direct projections from AI to the LA and BL, are clearly at variance with that proposal.

In the gerbil, there are strong projections from auditory cortex to the corpus striatum (CPu and GP; Fig. 9A–C), which mainly terminate in the caudal part of the CPu and in the caudomedial part of the GP. This is similar to what has been revealed in several species, such as rat (McGeorge & Faull, 1989; Roger & Arnault, 1989; Arnault & Roger, 1990; Moriizumi & Hattori, 1991; Rouiller & Welker, 1991; Vaudano *et al*., 1991; Romanski & LeDoux, 1993), cat (Diamond *et al*., 1969; Reale & Imig, 1983) and monkey (Forbes & Moskowitz, 1974; Yeterian & Pandya, 1998). On the other hand we could not demonstrate in the gerbil a field-specific and tonotopic organization of these projections to different loci of the CPu, as has been reported in macaque monkey (Yeterian & Pandya, 1998) and in cat (Reale & Imig, 1983).

In the gerbil, the fields AI, AAF, DP and VP project to the pontine nuclei (Fig. 11H–J), which are believed to be an integrating and relating centre between the cerebral and cerebellar cortices (for review see Ruigrok & Cella, 1995). Projections from auditory cortical fields to the pontine nuclei have also been reported in other rodents (e.g. Wiesendanger & Wiesendanger, 1982a,b; Azizi *et al*., 1985; Legg *et al*., 1989; Vaudano *et al*., 1991; Hofstetter & Ehret, 1992), rabbits (e.g. Knowlton *et al*., 1993) and cats (e.g. Diamond *et al*., 1969; Brodal, 1972).

Conclusions

The present study of the subcortical connections of the gerbil's four tonotopically organized auditory fields AI, AAF, DP and VP demonstrates that each field has a complex set of connections with various subcortical structures (Fig. 13). These include several nuclei of auditory pathways (MGB, IC, DNLL, MVPO, VNTB), visual pathways (DLG, LP, LD, SC), as well as multisensory (Rt, SG, PLi, pontine nuclei) and associative structures (amygdala, Corpus striatum). Projections from the auditory cortex to subcortical structures could constitute the anatomical basis for a cortical modulation of response properties of neurons in these structures. Although the investigated auditory fields AI, AAF, DP and VP share many of these connections, differences exist in the relative strength, and therefore probably in the descending influence, of each auditory cortical field. At the same time, however, a considerable overlap of functions in descending auditory processing is possible.

In the companion paper (Budinger *et al*., 2000) we provide evidence that the auditory cortex of the gerbil consists of at least core (AI and AAF) and noncore fields, suggested by field-specific cyto-, myelo- and chemoarchtitecture, corticocortical connections and physiological properties (e.g. Thomas *et al*., 1993). In the present study we have shown that each investigated field has its unique set of connections with tonotopic and nontonotopic auditory and various other sensory structures. Therefore, the core fields AI and AAF have the strongest connections with the tonotopically organized thalamus, namely MGv (e.g. Imig & Morel, 1984) and MGm (Rouiller *et al*., 1989). The noncore fields DP and VP have stronger projections to (and partly connections with) the nontonotopically organized auditory thalamus (MGd, SG, PLi) and to visual structures (LD, LP, DLG, SC). In addition, the projections from DP and VP to auditory brainstem structures (DNLL, SOC) are stronger than those from AAF and, if at all present, from AI. The organization of the gerbil's auditory cortex into a core and noncore and the field-specific connections with subcortical tonotopic and nontonotopic structures of the auditory modality and with structures of other modalities appears consistent with the concept of a hierarchical organization of auditory cortical processing on different levels in parallel tonotopic, nontonotopic and polysensory streams, as has been suggested for cats (Rouiller *et al*., 1991) and monkeys (Morel & Kaas, 1992; Morel *et al*., 1993; Pandya, 1995; Rauschecker *et al*., 1997; Hackett *et al*., 1998; Kaas & Hackett, 1998; Rauschecker, 1998). How auditory processing occurs at the various levels and streams remains to be further investigated.

Acknowledgements

We would like to thank A. Bolz, J. Stallmann, K. Baumann, C. Bucks and E. Müller as well as the other technical assistants for their excellent work, and Dr K. Richter for the helpful anatomical advice. This work was supported by a grant from Sachsen-Anhalt FKZ 2504 A/0086H.

Abbreviations

AAF, anterior auditory field; ac, anterior commissure; AI, primary auditory field; AStr, amygdalostriatal transition area; AV, anteroventral auditory field; AVCN, anteroventral cochlear nucleus; bic, brachium of the inferior colliculus; BL, basolateral amygdaloid nucleus; bsc, brachium of the superior colliculus; c, caudal; CA, central amygdaloid nucleus; CC, corpus callosum; CG, central grey; cic, commissure of the inferior colliculus; CIC, central nucleus of the inferior colliculus; CN, cochlear nuclei; cp, cerebral peduncle; CPO, caudal periolivary nucleus; CPu, caudate putamen; Cu, cuneiform nucleus; d, dorsal; (d)VNLL (dorsal part of the) ventral nucleus of the lateral lemniscus; D, dorsal auditory field; DCIC, dorsal cortex of the inferior colliculus; DCN, dorsal cochlear nucleus; DLG, dorsal lateral geniculate

nucleus; DLPO, dorsolateral periolivary nucleus; DMPO, dorsomedial periolivary nucleus; DNLL, dorsal nucleus of the lateral lemniscus; DP, dorsoposterior auditory field; DpG, deep grey layer of the superior colliculus; DPO, dorsal periolivary nucleus; ec, external capsule; ECIC, external cortex of the inferior colliculus; GP, globus pallidus; HF, hippocampal formation; ic, internal capsule; IC, inferior colliculus; InG, intermediate grey layer of the superior colliculus; INLL, intermediate nucleus of the lateral lemniscus; l, lateral; LA, lateral amygdaloid nucleus; LD, laterodorsal thalamic nucleus; LL (fibers of the) lateral lemniscus; LNTB, lateral nucleus of the trapezoid body; LP, lateral posterior thalamic nucleus; LSO, lateral superior olive; LV, lateral ventricle; LVPO, lateroventral periolivary nucleus; m, medial; MGB, medial geniculate nucleus (body); MGd, medial geniculate nucleus, dorsal division; MGm, medial geniculate nucleus, medial division; MGv, medial geniculate nucleus, ventral division; ml, medial lemniscus; MNTB, medial nucleus of the trapezoid body; MSO, medial superior olive; MVPO, medioventral periolivary nucleus; MZMG, marginal zone of the medial geniculate nucleus; NLL, nuclei of the lateral lemniscus; opt, optic tract; PLi, posterior limitans thalamic nucleus; Pn, pontine nuclei; Po, posterior thalamic nuclear group; Pta, pericollicular tegmental areas; PV, parvalbumin; PVCN, posteroventral cochlear nucleus; r, rostral; RPO, rostral periolivary nucleus; Rt, reticular thalamic nucleus; Sag, nucleus sagulum; SC, superior colliculus; SG, supragenículate nucleus; SOC, superior olivary complex; SPN, superior periolivary nucleus; str, superior thalamic radiation; SubG, subgeniculate nucleus; SuG, superficial grey layer of the superior colliculus; tb, trapezoid body; Te1-Te3, rat temporal cortex, area 1 (primary auditory cortex) to area 3; v, ventral; (v)VNLL (ventral part of the) ventral nucleus of the lateral lemniscus; V, ventral auditory field; VLG, ventral lateral geniculate nucleus; VM, ventromedial auditory field; VNTB, ventral nucleus of the trapezoid body; VP, ventroposterior auditory field; VPM, ventral posterior medial thalamic nucleus; ZI, zona incerta.

References

Aitkin, L.M., Kudo, M. & Irvine, D.R.F. (1988) Connections of the primary auditory cortex in the common marmoset, *Callithrix jacchus*. *J. Comp. Neurol.*, **269**, 235–248.

Amaral, D.G., Price, J.L., Pitkänen, A. & Carmichael, S.T. (1992) Anatomical organization of the primate amygdaloid complex. In Aggleton, J.P. (ed.), *The Amygdala: Neurobiological Aspects of Emotion, Memory, and Mental Dysfunction*. Wiley-Liss, New York, pp. 1–66.

Andersen, R.A., Knight, P.L. & Merzenich, M.M. (1980a) The thalamocortical and corticothalamic connections of AI, AII, and the anterior auditory field (AAF) in the cat: Evidence for two largely segregated systems of connections. *J. Comp. Neurol.*, **194**, 663–701.

Andersen, R.A., Snyder, R.L. & Merzenich, M.M. (1980b) The topographic organization of corticocollicular projections from physiologically identified loci in the AI, AII, and anterior auditory cortical fields of the cat. *J. Comp. Neurol.*, **191**, 479–494.

Arnault, P. & Roger, M. (1990) Ventral temporal cortex in the rat: Connections of secondary auditory areas Te2 and Te3. *J. Comp. Neurol.*, **302**, 110–123.

Azizi, S.A., Burne, R.A. & Woodward, D.J. (1985) The auditory corticopontocerebellar projection in the rat: inputs to the paraflocculus and midvermis. An anatomical and physiological study. *Exp. Brain Res.*, **59**, 36–49.

Bajo, V.M., Merchán, M.A., López, D.E. & Rouiller, E.M. (1993) Neuronal morphology and efferent projections of the dorsal nucleus of the lateral lemniscus in the rat. *J. Comp. Neurol.*, **334**, 241–262.

Braun, K. & Piepenstock, A. (1993) Parvalbumin-immunoreactive neurons in the subcortical auditory pathway of the Mongolian gerbil (*Meriones unguiculatus*). *Acta Histochem. Cytochem.*, **26**, 543–554.

Brawer, J.R., Morest, D.K. & Kane, E.C. (1974) The neuronal architecture of the cochlear nucleus of the cat. *J. Comp. Neurol.*, **155**, 251–300.

Brodal, P. (1972) The corticopontine projection in the cat. The projection from the auditory cortex. *Arch. Ital. Biol.*, **110**, 119–144.

Bronchti, G., Heil, P., Scheich, H. & Wollberg, Z. (1989) Auditory pathway and auditory activation of primary visual targets in the blind mole rat (*Spalax ehrenbergi*): I. 2-deoxyglucose study of subcortical centers. *J. Comp. Neurol.*, **284**, 253–274.

Brückner, S. & Rübsamen, R. (1995) Binaural response characteristics in isofrequency sheets of the gerbil inferior colliculus. *Hear. Res.*, **86**, 1–14.

Budinger, E. & Scheich, H. (1997) Auditory cortical and subcortical connections of the Mongolian gerbil. In Elsner, N. & Wässle, H. (eds), *Göttingen Neurobiology Report*. Georg Thieme-Verlag, Stuttgart, p. 699

Budinger, E., Heil, P. & Scheich, H. (2000) Functional organization of auditory cortex in the Mongolian gerbil (*Meriones unguiculatus*). III. Anatomical subdivisions and corticocortical connections. *Eur. J. Neurosci.,* **12**, 2425–2451.

Burton, H. & Jones, E.G. (1976) The posterior thalamic region and its cortical projection in New World and Old World monkeys. *J. Comp. Neurol.*, **168**, 249–301.

Caicedo, A., d'Aldin, C., Puel, J.L. & Eybalin, M. (1996) Distribution of calcium-binding protein immunoreactivities in the guinea pig auditory brainstem. *Anat. Embryol.*, **194**, 465–487.

Caird, D., Scheich, H. & Klinke, R. (1991) Functional organization of auditory cortical fields in the Mongolian gerbil (*Meriones unguiculatus*): Binaural 2-deoxyglucose patterns. *J. Comp. Physiol. A*, **168**, 13–26.

Cant, N.B. (1992) The cochlear nucleus: Neuronal types and their synaptic organization. In Webster, D.B., Popper, A.N. & Fay, R.R. (eds), *The Mammalian Auditory Pathway: Neuroanatomy*. Springer, New York, pp. 66–116.

Celio, M.R. (1990) Calbindin D-28k and parvalbumin in the rat nervous system. *Neuroscience*, **35**, 375–475.

Celio, M.R. & Heizmann, C.W. (1981) Calcium binding protein parvalbumin as a neuronal marker. *Nature*, **293**, 300–302.

Clarey, J.C., Barone, P. & Imig, T.J. (1992) Physiology of thalamus and cortex. In Popper, A.N., Fay, R.R. (eds), *The Mammalian Auditory Pathway: Neurophysiology*. Springer, New York, pp. 232–334.

Clerici, W.J. & Coleman, J.R. (1990) Anatomy of the rat medial geniculate body: I. Cytoarchitecture, myeloarchitecture, and neocortical connectivity. *J. Comp. Neurol.*, **297**, 14–31.

Coleman, J.R. & Clerici, W.J. (1987) Sources of projections to subdivisions of the inferior colliculus in the rat. *J. Comp. Neurol.*, **262**, 215–226.

Conley, M., Kupersmith, A.C. & Diamond, I.T. (1991) The organization of projections from subdivisions of the auditory cortex and thalamus to the auditory sector of the thalamic reticular nucleus in the *Galago*. *Eur. J. Neurosci.*, **3**, 1089–1103.

Crabtree, J.W. (1998) Organization in the auditory sector of the cat's thalamic reticular nucleus. *J. Comp. Neurol.*, **390**, 167–182.

de Venecia, R.K., Smelser, C.B., Lossman, S.D. & McMullen, N.T. (1995) Complementary expression of parvalbumin and calbindin D-28k delineates subdivisions of the rabbit medial geniculate body. *J. Comp. Neurol.*, **359**, 595–612.

de Venecia, R.K., Smelser, C.B. & McMullen, N.T. (1998) Parvalbumin is expressed in a reciprocal circuit linking the medial geniculate body and auditory neocortex in the rabbit. *J. Comp. Neurol.*, **400**, 349–362.

Diamond, I.T., Jones, E.G. & Powell, T.P.S. (1969) The projection of the auditory cortex upon the diencephalon and brain stem in the cat. *Brain Res.*, **15**, 305–340.

Druga, R. & Syka, J. (1984) Projections from auditory structures to the superior colliculus in the rat. *Neurosci. Lett.*, **45**, 247–252.

Echteler, S.M., Arjmand, E. & Dallos, P. (1989) Developmental alterations in the frequency map of the mammalian cochlea. *Nature*, **341**, 147–149.

Faye-Lund, H. (1985) The neocortical projections to the inferior colliculus in the albino rat. *Anat. Embryol.*, **173**, 53–70.

Faye-Lund, H. & Osen, K.K. (1985) Anatomy of the inferior colliculus in rat. *Anat. Embryol.*, **171**, 1–20.

Feliciano, M., Saldana, E. & Mugnaini, E. (1995) Direct projections from the rat primary auditory cortex to the nucleus sagulum, paralemniscal regions, superior olivary complex and cochlear nuclei. *Aud. Neurosci.*, **1**, 287–308.

Feng, J.J., Kuwada, S., Ostapoff, E.M., Batra, R. & Morest, D.K. (1994) A physiological and structural study of neuron types in the cochlear nucleus. I. Intracellular responses to acoustic stimulation and current injection. *J. Comp. Neurol.*, **346**, 1–18.

Fitzpatrick, K.A. & Imig, T.J. (1978) Projections of auditory cortex upon the thalamus and midbrain in the owl monkey. *J. Comp. Neurol.*, **177**, 537–556.

Forbes, B.F. & Moskowitz, N. (1974) Projections of auditory responsive cortex in the squirrel monkey. *Brain Res.*, **67**, 239–254.

Frisina, R.D., Smith, R.L. & Chamberlain, S.C. (1990) Encoding of amplitude modulation in the gerbil cochlear nucleus: I. A hierarchy of enhancement. *Hear. Res.*, **44**, 99–122.

Gallyas, F. (1979) Silver staining of myelin by means of physical development. *Neurol. Res.*, **1**, 203–209.

Gerfen, C.R. & Sawchenko, P.E. (1984) An anterograde neuroanatomical tracing method that shows the detailed morphology of neurons, their axons and terminals: immunohistochemical localization of an axonally transported plant lecitin, *Phaseolus vulgaris* Leucoagglutinin (PHA-L). *Brain Res.*, **290**, 219–238.

Glendenning, K.K., Brunso-Bechtold, J.K., Thompson, G.C. & Masterton,

R.B. (1981) Ascending auditory afferents to the nuclei of the lateral lemniscus. *J. Comp. Neurol.*, **197**, 673–703.
Hackett, T.A., Stepniewska, I. & Kaas, J.H. (1998) Thalamocortical connections of the parabelt auditory cortex in macaque monkeys. *J. Comp. Neurol.*, **400**, 271–286.
Hackney, C.M., Osen, K.K. & Kolston, J. (1990) Anatomy of the cochlear nuclear complex of guinea pig. *Anat. Embryol.*, **182**, 123–149.
Harris, D.M., Shannon, R.V., Snyder, R. & Carney, E. (1997) Multi-unit mapping of acoustic stimuli in gerbil inferior colliculus. *Hear. Res.*, **108**, 145–156.
Harrison, J.M. & Feldmann, M.L. (1970) Anatomical aspects of the cochlear nucleus and superior olivary complex. *Contrib. Sensory Physiol.*, **4**, 95–142.
Hashikawa, T., Molinari, M., Rausell, E. & Jones, E.G. (1995) Patchy and laminar terminations of the medial geniculate axons in monkey auditory cortex. *J. Comp. Neurol.*, **362**, 195–208.
Hashikawa, T., Raussell, E., Molinari, M. & Jones, E.G. (1991) Parvalbumin- and calbindin-containing neurons in the monkey medial geniculate complex: differential distribution and cortical layer specific projections. *Brain Res.*, **544**, 335–341.
Heil, P., Schulze, H. & Langner, G. (1995) Ontogenetic development of periodicity coding in the inferior colliculus of the Mongolian gerbil. *Aud. Neurosci.*, **1**, 363–383.
Helfert, R.H. & Schwartz, I.R. (1986) Morphological evidence for the existence of multiple neuronal classes in the cat lateral superior olivary nucleus. *J. Comp. Neurol.*, **244**, 533–549.
Helfert, R.H. & Schwartz, I.R. (1987) Morphological features of five neuronal classes in the gerbil lateral superior olive. *Am. J. Anat.*, **179**, 55–69.
Herbert, H., Aschoff, A. & Ostwald, J. (1991) Topography of projections from the auditory cortex to the inferior colliculus in the rat. *J. Comp. Neurol.*, **304**, 103–122.
Hess, A. & Scheich, H. (1996) Optical and FDG mapping of frequency-specific activity in auditory cortex. *Neuroreport*, **7**, 2643–2647.
Hicks, T.P., Stark, C.A. & Fletcher, W.A. (1986) Origins of afferents to visual suprageniculate nucleus of the cat. *J. Comp. Neurol.*, **246**, 544–554.
Hofstetter, K.M. & Ehret, G. (1992) The auditory cortex of the mouse: Connections of the ultrasonic field. *J. Comp. Neurol.*, **323**, 370–386.
Horikawa, J., Ito, S., Hosokawa, Y., Homma, T. & Murata, K. (1988) Tonotopic representation in the rat auditory cortex. *Proc. Jpn. Acad.*, **64**, :260–263.
Imig, T.J. & Morel, A. (1984) Topographic and cytoarchitectonic organization of thalamic neurons related to their targets in low, middle and high frequency representations in cat auditory cortex. *J. Comp. Neurol.*, **227**, 511–539.
Izzo, P.N. (1991) A note on the use of biocytin in anterograde tracing studies in the central nervous system: application at both light and electron microscopic level. *J. Neurosci. Meth*, **36**, 155–166.
Jones, E.G. (1975) Some aspects of the organization of the thalamic reticular complex. *J. Comp. Neurol.*, **162**, 285–308.
Jones, E.G. & Powell, T.P.S. (1971) An analysis of the posterior group of the thalamic nuclei on the basis of its afferent connections. *J. Comp. Neurol.*, **143**, 185–216.
Kaas, J.H. & Hackett, T.A. (1998) Subdivisions of auditory cortex and levels of processing in primates. *Audiol. Neurootol.*, **3**, 73–85.
Kane, E.S. & Barone, L.M. (1980) The dorsal nucleus of the lateral lemniscus in the cat: neuronal types and their distributions. *J. Comp. Neurol.*, **192**, 797–826.
Katoh, Y.Y. & Benedek, G. (1995) Organization of the colliculo-suprageniculate pathway in the cat: a wheat germ agglutinin–horseradish peroxidase study. *J. Comp. Neurol.*, **352**, 381–397.
King, M.A., Louis, P.M., Hunter, B.E. & Walker, D.W. (1989) Biocytin: a versatile anterograde neuroanatomical tract-tracing alternative. *Brain Res.*, **497**, 361–367.
Knowlton, B.J., Thompson, B.K. & Thompson, R.F. (1993) Projections from the auditory cortex to the pontine nuclei in the rabbit. Behav. *Brain Res.*, **56**, 23–30.
LeDoux, J.E. (1992) Emotion and the amygdala. In Aggleton, J.P. (ed), *The Amygdala: Neurobiological Aspects of Emotion, Memory, and Mental Dysfunction*. Wiley-Liss, New York, pp. 339–351.
Legg, C.R., Mercier, B. & Glickstein, M. (1989) Corticopontine projection in the rat: The distribution of labelled cortical cells after large injections of horseradish peroxidase in the pontine nuclei. *J. Comp. Neurol.*, **286**, 427–441.
Lohmann, C. & Friauf, E. (1996) Distribution of the calcium-binding proteins parvalbumin and calretinin in the auditory brainstem of adult and developing rats. *J. Comp. Neurol.*, **367**, 90–109.
Loskota, W.J., Lomax, P. & Verity, M.A. (1974) *A stereotaxic atlas of the Mongolian gerbil (Meriones Unguiculatus).* Ann Arbor Science, Michigan.
Luethke, L.E., Krubitzer, L.A. & Kaas, J.H. (1989) Connections of primary auditory cortex in the new world monkey *Saguinus. J. Comp. Neurol.*, **285**, 487–513.
Mascagni, F., McDonald, A.J. & Coleman, J.R. (1993) Corticoamygdaloid and corticocortical projections of the rat temporal cortex: a *Phaseolus vulgaris* leucoagglutinin study. *Neuroscience*, **57**, 697–715.
McDonald, A.J. (1992) Neuroanatomical labeling with biocytin: a review. *Neuroreport*, **3**, 821–827.
McDonald, A.J. (1998) Cortical pathways to the mammalian amygdala. *Prog. Neurobiol.*, **55**, 257–332.
McGeorge, A.J. & Faull, R.L.M. (1989) The organization of the projection from the cerebral cortex to the striatum in the rat. *Neuroscience*, **29**, 503–537.
McMullen, N.T. & de Venecia, R.K. (1993) Thalamocortical patches in auditory neocortex. *Brain Res.*, **620**, 317–322.
McMullen, N.T., Smelser, C.B. & de Venecia, R.K. (1994) A quantitative analysis of parvalbumin neurons in rabbit auditory neocortex. *J. Comp. Neurol.*, **349**, 493–511.
Meredith, M.A. & Clemo, H.R. (1989) Auditory cortical projection from the anterior ectosylvian sulcus (Field AES) to the superior colliculus in the cat: an anatomical and electrophysiological study. *J. Comp. Neurol.*, **289**, 687–707.
Mitani, A., Itoh, K. & Mizuno, N. (1987) Distribution and size of thalamic neurons projecting to layer I of the auditory cortical fields of the cat compared to those projecting to layer IV. *J. Comp. Neurol.*, **257**, 105–121.
Molinari, M., Dell'Anna, M.E., Rausell, E., Leggio, M.G., Hashikawa, T. & Jones, E.G. (1995) Auditory thalamocortical pathways defined in monkeys by calcium-binding protein immunoreactivity. *J. Comp. Neurol.*, **362**, 171–194.
Morel, A., Garraghty, P.E. & Kaas, J.H. (1993) Tonotopic organization, architectonic fields, and connections of auditory cortex in macaque monkeys. *J. Comp. Neurol.*, **335**, 437–459.
Morel, A. & Imig, T.J. (1987) Thalamic projections to fields A, AI, P and VP in the cat auditory cortex. *J. Comp. Neurol.*, **265**, 119–144.
Morel, A. & Kaas, J.H. (1992) Subdivisions and connections of auditory cortex in owl monkeys. *J. Comp. Neurol.*, **318**, 27–63.
Morest, D.K. (1968) The collateral system of the medial nucleus of the trapezoid body of the cat, its neuronal architecture and relation to the olivo-cochlear bundle. *Brain Res.*, **9**, 288–311.
Morest, D.K. & Oliver, D.L. (1984) The neuronal architecture of the inferior colliculus in the cat: defining the functional anatomy of the auditory midbrain. *J. Comp. Neurol.*, **222**, 209–236.
Moreu, R., Berna, A.R., Pico, M.L., Beneyto, M. & Prieto, J.J. (1999) Are the connections between the auditory cortical areas and the amygdaloid complex hierarchically organized? *Soc. Neurosci. Abstr.,* **25**, 1420.
Moriizumi, T. & Hattori, T. (1991) Pyramidal cells in rat temporoauditory cortex project to both striatum and inferior colliculus. *Brain Res. Bull.*, **27**, 141–144.
Müller, M. (1996) The cochlear place-frequency map of the adult and developing Mongolian gerbil. *Hear. Res.*, **94**, 148–156.
National Research Council. Institute of Laboratory Animal Resources. Commission on Life Sciences. (1996) *NIH Guide for the Care and Use of Laboratory Animals.* National Academy Press, Washington, DC.
Oliver, D.L. & Hall, W.C. (1978a) The medial geniculate body of the tree shrew, *Tupaia glis*. I. Cytoarchitecture and midbrain connections. *J. Comp. Neurol.*, **182**, 423–458.
Oliver, D.L. & Hall, W.C. (1978b) The medial geniculate body of the tree shrew, *Tupaia glis*. II. Connections with the neocortex. *J. Comp. Neurol.*, **182**, 459–493.
Oliver, D.L. & Huerta, M.F. (1992) Inferior and superior colliculi. In Webster, D.B., Popper, A.N. & Fay, R.R. (eds), *The Mammalian Auditory Pathway: Neuroanatomy*. Springer, New York, pp. 168–221.
Oliver, D.L. & Morest, D.K. (1984) The central nucleus of the inferior colliculus in the cat. *J. Comp. Neurol.*, **222**, 237–264.
Osen, K.K. (1969) Cytoarchitecture of the cochlear nuclei in the cat. *J. Comp. Neurol.*, **136**, 453–484.
Ostapoff, E.M., Feng, J.J. & Morest, D.K. (1994) A physiological and structural study of neuron types in the cochlear nucleus. II. Neuron types and their structural correlation with response properties. *J. Comp. Neurol.*, **346**, 19–42.
Pandya, D.N. (1995) Anatomy of the auditory cortex. *Rev. Neurol. (Paris)*, **151**, 486–494.
Pandya, D.N., Rosene, D.L. & Doolittle, A.M. (1994) Corticothalamic

connections of auditory-related areas of the temporal lobe in the rhesus monkey. *J. Comp. Neurol.*, **345**, 447–471.
Paula-Barbosa, M.M. & Sousa-Pinto, A. (1973) Auditory cortical projections to the superior colliculus in the cat. *Brain Res.*, **50**, 47–61.
Paxinos, G. (1995). *The Rat Nervous System*. Academic Press, Sydney.
Paxinos, G. & Watson, C. (1986). *The Rat Brain in Stereotaxic Coordinates*. Academic Press, Sydney.
Rauschecker, J.P. (1998) Parallel processing in the auditory cortex of primates. *Audiol. Neurootol.*, **3**, 86–103.
Rauschecker, J.P., Tian, B., Pons, T. & Mishkin, M. (1997) Serial and parallel processing in rhesus monkey auditory cortex. *J. Comp. Neurol.*, **382**, 89–103.
Reale, R.A. & Imig, T.J. (1983) Auditory cortical field projections to the basal ganglia of the cat. *Neuroscience*, **8**, 67–86.
Redies, H., Brandner, S. & Creutzfeldt, O.D. (1989) Anatomy of the auditory thalamocortical system of the guinea pig. *J. Comp. Neurol.*, **282**, 489–511.
Richter, K., Hess, A. & Scheich, H. (1999) Functional mapping of transsynaptic effects of local manipulation of inhibition in gerbil auditory cortex. *Brain Res.*, **831**, 184–199.
Rockel, A.J. & Jones, E.G. (1973a) The neuronal organization of the inferior colliculus of the adult cat. I. The central nucleus. *J. Comp. Neurol.*, **147**, 11–60.
Rockel, A.J. & Jones, E.G. (1973b) The neuronal organization of the inferior colliculus of the adult cat. II. The pericentral nucleus. *J. Comp. Neurol.*, **149**, 301–334.
Roger, M. & Arnault, P. (1989) Anatomical study of the connections of the primary auditory area in the rat. *J. Comp. Neurol.*, **287**, 339–356.
Romanski, L.M. & LeDoux, J.E. (1993) Information cascade from primary auditory cortex to the amygdala: Corticocortical and corticoamygdaloid projections of the temporal cortex in the rat. *Cereb. Cortex*, **3**, 515–532.
Rouiller, E.M., Colomb, E., Capt, M. & de Ribaupierre, F. (1985) Projections of the reticular complex of the thalamus onto physiologically characterized regions of the medial geniculate body. *Neurosci. Lett.*, **53**, 227–232.
Rouiller, E.M., Rodrigues- Dagaeff, C., Simm, G., de Ribaupierre, R.Y., Villa, A. & de Ribaupierre, F. (1989) The functional organization of the medial division of the medial geniculate body of the cat: tonotopic organization, spatial distribution of response properties and cortical connections. *Hear. Res.*, **39**, 127–142.
Rouiller, E.M., Simm, G.M., Villa, A.E.P., de Ribaupierre, Y. & de Ribaupierre, F. (1991) Auditory corticocortical interconnections in the cat: Evidence for parallel and hierarchical arrangement of the auditory cortical areas. *Exp. Brain Res.*, **86**, 483–503.
Rouiller, E.M. & Welker, E. (1991) Morphology of corticothalamic terminals arising from the auditory cortex of the rat: a Phaseolus vulgaris-leucoagglutinin (PHA-L) tracing study. *Hear. Res.*, **56**, 179–190.
Ruigrok, T.J.L. & Cella, F. (1995) Precerebellar nuclei and red nucleus. In Paxinos, G. (ed.), *The Rat Nervous System*. Academic Press, Sydney, pp. 277–308.
Ryugo, D.K. & Weinberger, N.M. (1976) Corticofugal modulation of the medial geniculate body. *Exp. Neurol.*, **51**, 377–391.
Sally, S.L. & Kelly, J.B. (1988) Organization of auditory cortex in the albino rat: sound frequency. *J. Neurophysiol.*, **59**, 1627–1638.
Scheel, M. (1988) Topographic organization of the auditory thalamocortical system in the albino rat. *Anat. Embryol.*, **179**, 181–190.
Scheich, H., Heil, P. & Langner, G. (1993) Functional organization of auditory cortex in the Mongolian gerbil (*Meriones unguiculatus*). II. Tonotopic 2-Deoxyglucose. *Eur. J. Neurosci.*, **5**, 898–914.
Schofield, B.R. & Cant, N.B. (1991) Organization of the superior olivary complex in the guinea pig. I. Cytoarchitecture, cytochrome oxidase histochemistry, and dendritic morphology. *J. Comp. Neurol.*, **314**, 645–670.
Schofield, B.R. & Cant, N.B. (1997) Ventral nucleus of the lateral lemniscus in guinea pigs: cytoarchitecture and inputs from the cochlear nucleus. *J. Comp. Neurol.*, **379**, 363–385.
Schwartz, I.R. (1977) Dendritic arrangements in the cat medial superior olive. *Neuroscience*, **2**, 81–101.
Schwartz, I.R. (1992) The superior olivary complex and lateral lemniscal nuclei. In Webster, D.B., Popper, A.N. & Fay, R.R. (eds), *The Mammalian Auditory Pathway: Neuroanatomy*. Springer, New York, pp. 117–167.
Seto-Ohshima, A., Aoki, E., Omori, A., Mizutani, A., Murashima, Y. & Heizmann, C.W. (1994) Parvalbumin immunoreactivity and cytochrome oxidase activity in the brain of the Mongolian gerbil. *Acta Histochem. Cytochem.*, **27**, 309–321.
Shi, C.J. & Cassell, M.D. (1997) Cortical, thalamic, and amygdaloid projections of rat temporal cortex. *J. Comp. Neurol.*, **382**, 153–175.
Spitzer, M.W. & Semple, M.N. (1991) Interaural phase coding in auditory midbrain: influence of dynamic stimulus features. *Science*, **254**, 721–724.
Spitzer, M.W. & Semple, M.N. (1995) Neurons sensitive to interaural phase disparity in gerbil superior olive: diverse monaural and temporal response properties. *J. Neurophysiol.*, **73**, 1668–1690.
Steffen, H., Simonis, C., Thomas, H., Tillein, J. & Scheich, H. (1988) Auditory cortex: Multiple fields, their architectonics and connections in the Mongolian gerbil. In Syka, J. & Masterton, R.B. (eds), *Auditory Pathway*. Plenum, New York, pp. 223–228.
Sugimoto, S., Sakurada, M., Horikawa, J. & Taniguchi, I. (1997) The columnar and layer-specific response properties of neurons in the primary auditory cortex of Mongolian gerbils. *Hear. Res.*, **112**, 175–185.
Takahashi, T. (1985) The organization of the lateral thalamus of the hooded rat. *J. Comp. Neurol.*, **231**, 281–309.
Thomas, H., Tillein, J., Heil, P. & Scheich, H. (1993) Functional organization of auditory cortex in the Mongolian gerbil (*Meriones unguiculatus*). I. Electrophysiological mapping of frequency representation and distinction of fields. *Eur. J. Neurosci.*, **5**, 882–897.
Thompson, S.M. & Robertson, R.T. (1987a) Organization of subcortical pathways for sensory projections to the limbic cortex. I. Subcortical projections to the medial limbic cortex in the rat. *J. Comp. Neurol.*, **265**, 175–188.
Thompson, S.M. & Robertson, R.T. (1987b) Organization of subcortical pathways for sensory projections to the limbic cortex. II. Afferent projections to the thalamic lateral dorsal nucleus in the rat. *J. Comp. Neurol.*, **265**, 189–202.
Van Groen, T. & Wyss, J.M. (1992) Projections from the laterodorsal nucleus of the thalamus to the limbic and visual cortices in the rat. *J. Comp. Neurol.*, **324**, 427–448.
Vaudano, E., Legg, C.R. & Glickstein, M. (1991) Afferent and efferent connections of temporal association cortex in the rat: a horseradish peroxidase study. *Eur. J. Neurosci.*, **3**, 317–330.
Villa, A.E.P. (1990) Physiological differentiation within the auditory part of the thalamic reticular nucleus of the cat. *Brain Res. Rev.*, **15**, 25–40.
Villa, A.E.P., Rouiller, E.M., Simm, G.M., Zurita, P., de Ribaupierre, Y. & de Ribaupierre, F. (1991) Cortifugal modulations of the information processing in the auditory thalamus of the cat. *Exp. Brain Res.*, **86**, 506–517.
Weedman, D.L. & Ryugo, D.K. (1996) Pyramidal cells in primary auditory cortex project to the cochlear nucleus in rat. *Brain Res.*, **706**, 97–102.
Wiesendanger, R. & Wiesendanger, M. (1982a) The corticopontine system in the rat. I. Mapping of corticopontine neurons. *J. Comp. Neurol.*, **208**, 215–226.
Wiesendanger, R. & Wiesendanger, M. (1982b) The corticopontine system in the rat. II. The projection pattern. *J. Comp. Neurol.*, **208**, 227–238.
Winer, J.A. (1985) The medial geniculate body of the cat. *Adv. Anat. Embryol. Cell Biol.*, **86**, 1–97.
Winer, J.A. (1992) The functional architecture of the medial geniculate body and the primary auditory cortex. In Webster, D.B., Popper, A.N. & Fay, R.R. (eds), *The Mammalian Auditory Pathway: Neuroanatomy*. Springer, New York, pp. 222–409.
Winer, J.A., Diamond, I.T. & Raczkowski, D. (1977) Subdivisions of the auditory cortex of the cat: The retrograde transport of horseradish peroxidase to the medial geniculate body and posterior thalamic nuclei. *J. Comp. Neurol.*, **176**, 387–418.
Winer, J.A., Kelly, J.B. & Larue, D.T. (1999a) Neural architecture of the rat medial geniculate body. *Hear. Res.*, **130**, 19–41.
Winer, J.A. & Larue, D.T. (1987) Patterns of reciprocity in auditory thalamocortical and corticothalamic connections: Study with horseradish peroxidase and audioradiographic methods in the rat medial geniculate body. *J. Comp. Neurol.*, **257**, 282–315.
Winer, J.A., Larue, D.T., Diehl, J.J. & Hefti, B.J. (1998) Auditory cortical projections to the cat inferior colliculus. *J. Comp. Neurol.*, **400**, 147–174.
Winer, J.A., Kelly, J.B. & Larue, D.T. (1999a) Neural architecture of the rat medial geniculate body. *Hear. Res.*, **130**, 19–41.
Winer, J.A., Sally, S.L., Larue, D.T. & Kelly, J.B. (1999b) Origins of medial geniculate body projections to physiologically defined zones of rat primary auditory cortex. *Hear. Res.*, **130**, 42–61.
Yan, W. & Suga, N. (1998) Corticofugal modulation of the midbrain frequency map in the bat auditory system. *Nature Neurosci.*, **1**, 54–58.
Yeterian, E.H. & Pandya, D.N. (1998) Corticostriatal connections of the superior temporal region in rhesus monkeys. *J. Comp. Neurol.*, **399**, 384–402.